communications biology

A Nature Portfolio journal

Article

https://doi.org/10.1038/s42003-025-08586-8

A multi-tissue human knee single-cell atlas identifies that osteoarthritis reduces regenerative tissue stem cells while increasing inflammatory pain macrophages

Rajnikant Dilip Raut[1], Amit Kumar Chakraborty[1], Tuhina Neogi[2], Michael Albro[3,4], Brian Snyder[5,6], Thomas P. Schaer[7], Chao Zhang[8], Mark W. Grinstaff[9] & Manish V. Bais[1]

Osteoarthritis (OA) affects the entire knee joint, yet cross-tissue molecular interplay remains poorly understood. To address this, we constructed the first single-cell RNA sequencing atlas of knee OA, profiling articular cartilage, meniscus, synovium, and subchondral bone. Our analysis revealed that healthy synovium and meniscus harbor abundant tissue stem cells (TSCs) and immune cells, which are significantly altered in OA. Regenerative TSCs expressing SDF1, SOX9, CD146, PDGFRB, and CD105 are reduced, while osteogenic TSCs marked by *NT5E* are expanded. OA cartilage has distinct MMP13-producing detrimental chondrocytes while increasing *RUNX2*-producing chondrocytes and fibroblasts. OA tissues are enriched with inflammatory (*IL1B-IL6-NOS2-TNF*) and pain-marker (*P2RX7*)-specific macrophages, inflammatory genes expression and immune cells. Cell-cell communication contributes to OA progression, promotes proinflammatory macrophages, and osteogenic TSCs. By identifying these OA-specific cells and molecular interplay, and constructing the first multi-tissue comprehensive atlas, we bridge the critical knowledge gaps and lay the foundation for advancing targeted OA therapies.

Osteoarthritis (OA) is a chronic joint condition affecting over 520 million adults worldwide. It causes pain, swelling, and reduced joint movements. The annual treatment costs, both direct and indirect, are nearly $486.4 billion annually[1]. Our group has conducted several preclinical studies to target OA mechanisms[2–4]. The pathophysiology of OA includes various biochemical[5–8], biomechanical[9–11], metabolic[12], and gene-regulated[13] mechanisms. The cellular and molecular heterogeneity underlying human clinical OA remains incompletely understood owing to the lack of a multi-tissue OA atlas. Therefore, we constructed the first comprehensive single-cell atlas of a human knee affected by OA. Our goal was to identify different cell types and to understand their roles in OA development. We studied cartilage, synovium, subchondral bone (SCB), and meniscal tissue. We evaluated specific cell types, including stem cells, macrophages, and other immune cells, which play key roles in inflammation and tissue remodeling.

Mechanical overloading or biomechanical changes[14] can lead to structural tissue failure (fissuring/fibrillation),[15] tissue swelling[16], compositional loss of glycosaminoglycans (GAG)[17], and derangement of the COLII network[18]. Mechanical injury also induces an inflammatory response and elevated cytokine levels in the OA synovial fluid (e.g., IL-1B, TNF-α)[19,20]. Depletion of cartilage GAG diminishes its rheological and tribological

[1]Translational Dental Medicine, Boston University Henry M. Goldman School of Dental Medicine, Boston, MA, USA. [2]Section of Rheumatology, Boston University Chobanian & Avedisian School of Medicine, Boston, MA, USA. [3]Department of Mechanical Engineering, Boston University, Boston, Massachusetts, MA, USA. [4]Division of Materials Science & Engineering, Boston University, Boston, Massachusetts, MA, USA. [5]Musculoskeletal Translational Innovation Initiative, Carl J. Shapiro Department of Orthopaedic Surgery, Beth Israel Deaconess Medical Center, Harvard Medical School, Boston, MA, USA. [6]Department of Orthopaedic Surgery, Boston Children's Hospital, Harvard Medical School, Boston, MA, USA. [7]Department of Clinical Studies New Bolton Center, University of Pennsylvania School of Veterinary Medicine, Kennett Square, PA, USA. [8]Section of Computational Biomedicine, Boston University Chobanian & Avedisian School of Medicine, Boston, MA, USA. [9]Departments of Biomedical Engineering and Chemistry, Boston University, Boston, MA, USA. e-mail: bmanish@bu.edu

properties[21], independently contributing to the propagation of OA pathophysiology[22,23]. Joint kinematic dysfunction due to trauma, obesity, or lifelong use is one of the main risk factors of OA[24]. The resulting increased mechanical stress causes injury to the principal load-bearing tissues of the knee joint, meniscus, and cartilage[25] as well as to the synovium and SCB. Damage to even one of these tissues leads to a cascade of alterations in the other tissues, emphasizing the interrelated nature of joint tissue degeneration in OA. OA affects all knee joint tissues, including cartilage, menisci, synovium, and subchondral bone[26]. Despite this inter-tissue dependence, studies have typically focused on individual tissue types, such as cartilage[27], cartilage and meniscus[28], synovium and infrapatellar fat pad[29], and SCB[30], mainly omitting the underlying cross-tissue comm. Recent developments in single-cell RNA sequencing (scRNA-seq) and genomic technologies have provided insights into the crosstalk between cells in tissues and nearby tissues. As OA is an entire joint disease, the analysis of knee joint tissues, including cartilage, meniscus, synovium, and SCB, and their interaction at the single-cell level, is of interest and may provide an understanding of knee OA development.

A dysregulated balance between tissue degeneration and regeneration in the joint leads to OA pathology governed by tissue stem cells (TSCs). TSCs are a population of resident cells within a tissue that have two distinguishing characteristics: the ability to self-renew over time and the ability to develop into the major cell types within the tissue[31,32]. These cells are essential for maintaining tissue homeostasis and facilitating tissue repair after injury[32]. TSCs perform specific functions, and various types of TSCs are enriched in the synovium, meniscus, and cartilage. Studies have identified Numerous chondroprogenitor and stem cell markers expressed in TSCs[33–35]. Stem cells differentiate into chondrocytes during OA[36] and have the potential to repair cartilage repair[37]. The distinction between various TSCs can help to evaluate the balance of a specific pool. TSCs expressing regenerative factors can be categorized as regenerative TSCs. Osteogenic TSCs express factors related to osteogenic differentiation, inflammation, and OA. The TSC pool can be dysregulated by OA, injury, or inflammation.

In this study, we constructed an atlas of human knee single-cell transcriptomic profiles. We observed changes in specific stem cells, macrophages, and chondrocytes. We present a scRNA-seq atlas of 53 human knee joint samples from cartilage, meniscus, synovium, and SCB cells. Integrated analysis revealed OA-specific cell type clusters and showed how different tissues are related. The analysis included: 1) the effect and balance of TSCs during healthy and OA conditions; 2) Enrichment of MMP13-or catabolic factor-expressing chondrocytes, proinflammatory macrophages expressing quadruple positive markers (*IL1B-IL6-NOS2-TNF* +), and pain markers, such as *P2RX7*; and 3) identification of co-relative cellular associations for future translation. This knee joint scRNA-seq atlas provides a detailed examination of tissue-specific factors. This highlights the possible interactions between different cells in the nearby synovial tissue. These interactions could serve as targets for treatments aimed at reducing OA. This atlas helped us to identify important cell types and molecular aberrations in OA. These findings indicate possible therapeutic targets. This study is a big step toward understanding the complex etiology of human knee OA and opens new avenues for future research and therapeutic strategies.

Methods

Human healthy and OA knee specimens

With prior consent from the patients, samples of cartilage, meniscus, synovium & infrapatellar fat pad (SynoFP), and SCB from healthy individuals and OA patients were collected from the NCBI Gene Expression Omnibus (GEO) database (Fig. 1a). The sample description and corresponding accession IDs show the specific characteristics of the entire knee joint. The GEO Series (GSE) identifies the individual accession ID under which the raw sequencing data files are publicly available (Fig. 1a).

- GSE220243. Healthy cartilage ($n = 6$) and meniscal ($n = 7$) samples were obtained from the same knees. Cartilage samples were collected from the weight-bearing medial femoral condyle (the entire meniscus). OA cartilage samples ($n = 6$) were collected from the medial femoral condyle osteochondral slabs; meniscus samples ($n = 6$) were excluded from those with large calcium deposits[28].
- The GSE169454 OA cartilage samples ($n = 4$) were extracted from patients undergoing total knee arthroplasty for OA. Non-arthritic femoral condyle cartilage specimens ($n = 3$) were collected from fresh osteochondral allograft remnants discarded after osteochondral allograft surgical reconstructions[38].
- GSE255460 cartilage samples were collected from eight patients with OA who underwent total knee arthroplasty and three non-OA who underwent above-knee amputation with no prior history of joint injury or disease[39].
- GSE216651 SynoFP samples were obtained from three individuals with end-stage knee OA who underwent total knee arthroplasty. Non-OA SynoFP biopsies were obtained from three patients who underwent excision of bone tumors surrounding the knee joint or from organ transplant donors[29].
- GSE196678 SCB samples were isolated from the medial and lateral tibial plateaus of two patients with OA undergoing total knee arthroplasty. Patients were divided into two groups: non-OA ($n = 2$) from the lateral tibial plateau and OA ($n = 2$) from the medial side[30].

Briefly, all healthy samples from the cartilage, meniscus, SynoFP, and SCB were processed individually for quality control and doublets and integrated using the harmony integration method in Seurat. Similarly, all OA samples were processed and subjected to CellChat[40] and pseudotime trajectory analysis (Fig. 1b, c). Finally, for comparative analysis, both preprocessed healthy and OA samples were integrated and subjected to clustering, cell identity, and cell type proportion analysis (Fig. 1d). This was followed by extraction of macrophages and TSCs for downstream analyses. As shown in Fig. 1b and c, 130012 cells from healthy and 195742 cells from OA cells were retained after quality control and preprocessing. The total number of cells retained from each tissue type was analyzed (Fig. 1b, c).

Quality control and preprocessing

Individual files of Healthy and OA patients and single-cell RNA sequencing (scRNA-seq) for knee joint cartilage, meniscus, SynoFP, and SCB were downloaded from NCBI GEO and processed independently. The zipped files contained a count matrix, features (genes), and barcode files, which were imported into R studio and converted to a Seurat object using the *CreateSeuratObject* function in the Seurat R package (v5.1.0)[41] with no initial cutoffs. Further details regarding sample characterization and categorization are described.

To filter out low-quality cells, we eliminated cells with less than 3000 RNA counts, 400 genes (features) detected, and more than 10% of the reads originated from mitochondrial genes. The retained high-quality cells were further normalized using the default *LogNormalize* method and a scale factor of 10,000 within *NormalizeData* function of Seurat. Clustering was performed with 20 Principal Components (PCs) at a resolution of 0.5, using 2000 variable features found using *FindVariableFeatures* with the "vst" selection method. The criteria for selecting PCs were defined using elbow plots. Next, *DoubletFinder* R package (v2.0.4) was used to eliminate doublet cells[42]. After quality control and preprocessing 130012 cells from healthy and 195742 cells from OA cells were retained.

Data Integration and cluster identification

All the individually processed files were combined into a single Seurat object. The combined files were subjected to data integration using *HarmonyIntegration*[43] method within *IntegrateLayers* function of Seurat[44]. For downstream processing, 20 PCs were used for harmony clustering at a 0.5 resolution. Healthy samples were combined to determine the cellular and molecular landscapes. The OA samples were combined to understand the cellular and molecular landscapes. Both Healthy and OA samples were integrated to identify common and unique molecular events.

a

Knee Tissue Type	accession ID	Total Sample (n)	Age (years)	Gender (M/F)	Trait	Grading System	Grade	Species
Cartilage	GSE220243	6	20-56	5M/2F	non-OA	Outerbridge	0 or 1	Human
	GSE220243	6	61-86	2M/4F	OA	Outerbridge	4	Human
	GSE169454	3	Undisclosed	Undisclosed	non-OA	NA	NA	Human
	GSE169454	4	Undisclosed	Undisclosed	OA	Kellgren-Lawrence	3 or 4	Human
	GSE255460	3	46-55	2M/1F	non-OA	Outerbridge	Undisclosed	Human
	GSE255460	8	51-75	4M/4F	OA	Outerbridge	Undisclosed	Human
Meniscus	GSE220243	7	20-56	5M/2F	non-OA	Outerbridge	0 or 1	Human
	GSE220243	6	61-86	2M/4F	OA	Outerbridge	4	Human
Synovium & Fat pad	GSE216651	3	21-37	2M/1F	non-OA	Undisclosed	Undisclosed	Human
	GSE216651	3	64-82	3F	OA	Undisclosed	Undisclosed	Human
Subchondral bone	GSE196678	2	72-74	2F	non-OA	NA	NA	Human
	GSE196678	2	72-74	2F	OA	KSS score	54-58	Human

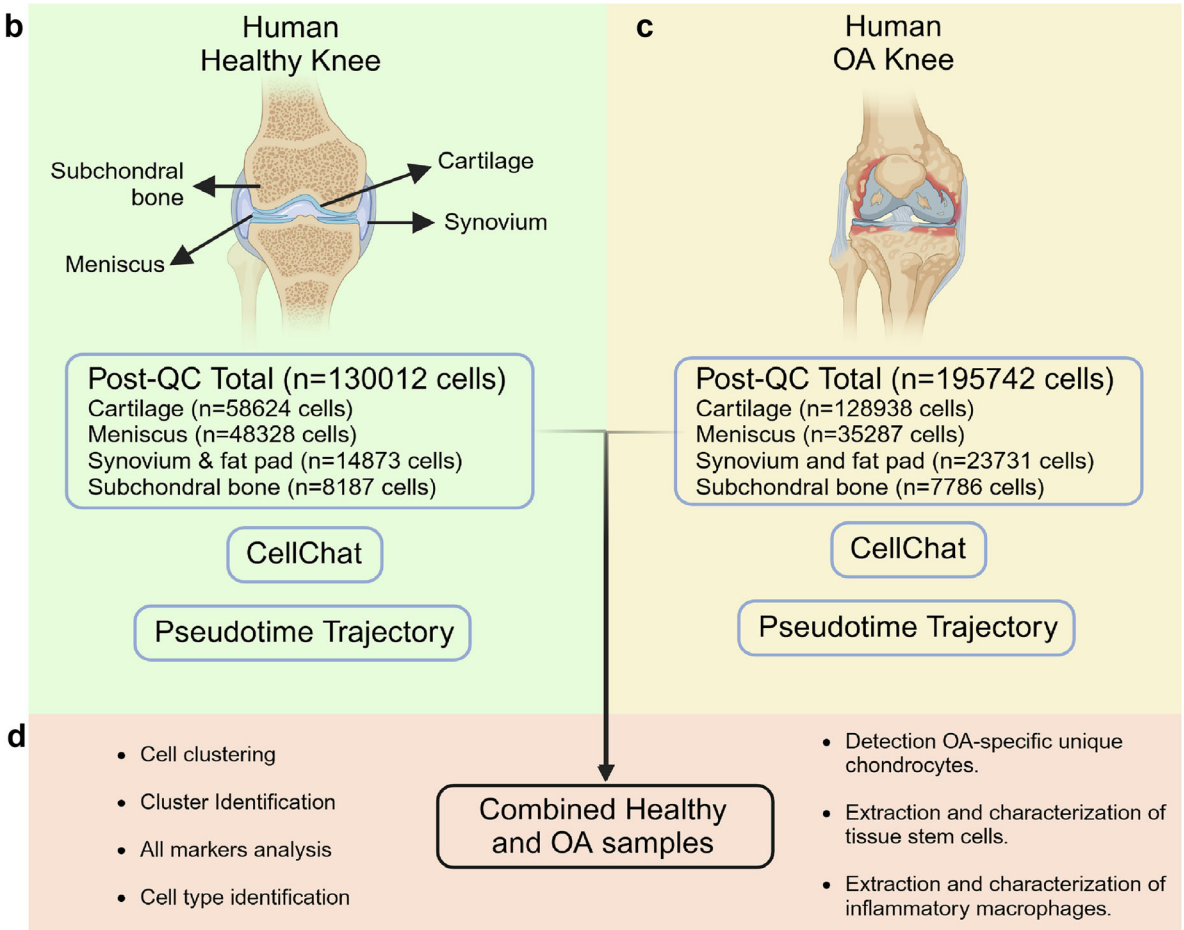

Fig. 1 | Sample characteristics and study overview. a Characteristic details of scRNA-seq samples used in this study. **b** Anatomy of the healthy human knee and the number of cells retained post-QC using standard Seurat and doubletFinder. **c** Anatomy of OA knee and the number of cells retained post-QC. **d** Overview of healthy and OA sample integration followed by downstream analyses.

Differential marker analysis, cell type identification, and gene set enrichment analysis (GSEA)

The *JoinLayers* function was used to merge all integrated layers. We performed differential expression analysis using *FindAllMarkers* function to identify the differentially expressed marker genes in each harmony cluster, as well as the markers of all four tissues. The Wilcoxon rank-sum test (Wilcox) was used to perform the analysis with *logfc.threshold* of 0.25, and the singleR (v2.8.0) and celldex (v1.16.0) R packages were used to identify the cell types. *HumanPrimaryCellAtlasData* from Celldex was considered for this study because it includes almost all cell types, including stem and immune cells[45,46]. TSCs and Macrophages were extracted using *a subset* function of Base R for downstream analyses. GSEA (v4.4.0) was performed

to investigate the highly enriched gene sets within each tissue type under normal and OA conditions.

Cell type proportion analysis

To evaluate the cell-type distribution across situations, cell metadata from the integrated Seurat object were extracted. Cell type proportions were computed by categorizing cells according to the identified cell types and experimental conditions and then normalized to obtain relative frequencies. A stacked bar plot was created using ggplot2 to show the proportion of each cell type per condition. Custom color mapping ensured that cell types were consistently represented across all samples. This technique allowed the detection of differences in cellular composition between healthy and OA conditions.

CellChat analysis

CellChat (v2.1.2) was run on the RNA data slot and separately on healthy and OA samples[40,47]. Overexpressed genes were identified using default parameters of *identifyOverExpressedGenes* function. Communication probabilities were computed using trim = 0.1, type = triMean, and other default parameters of *computeCommunProb* function. Communications were filtered to include those with at least 100 cells. The two cell-chat objects were merged to compare their interaction occurrences and strengths. *CommunProbPathway* function detects actively communicating signaling pathways. Data were visualized in a chord diagram, heatmaps, and scatter plots using the corresponding functional commands of the CellChat package.

Pseudotime trajectory analysis

Pseudo-trajectories of chondrocytes and TSCs were constructed using Monocle3[48]. The Seurat object was converted to a monocle3 cell_data_set object using *as.cell_data_set* function and preprocessed; 20 PCs were retained using the PCA method. Dimensionality reduction was performed using the UMAP method and was clustered using the cluster_ cell function. The *learn_graph* function was used to learn and build the trajectory. O*rder_cells* and *pseudotime* functions were used to order cells at pseudotime. Root nodes were selected from the TSCs cluster, considering chondroprogenitor cells as part of the TSCs.

NicheNet analysis

NicheNet analysis was performed in R to predict ligand-receptor interactions between the sender and receiver cell types. Single-cell RNA-seq data from healthy and OA patients were combined to identify sender (fibroblasts, chondrocytes, tissue stem cells, and macrophages) and receiver (macrophages and tissue stem cells) populations. The *nichenetr* package (version 2.2.0)[49] was used, which included ligand-receptor and signaling networks. Expressed genes were filtered using a minimum expression threshold (expression in at least 5% of cells) and differentially expressed genes in recipient cells were identified ($p\_val\_adj < 0.05$; $avg\_log2FC > 0.25$). Potential ligands from sender cells were ranked according to their regulatory potential for target genes. Visualization and downstream interpretation were conducted using built-in functions.

Data visualization

Uniform Manifold Approximation and Projection (UMAP) was used to visualize single-cell data. Violine plots, heatmaps, feature plots, and bar plots were generated using *vlnplot* (Seurat), *netAnalysis_signalingRole_heatmap* (CellChat), *Featureplot* (Seurat), and *ggplot2* functions, respectively.

Reporting summary

Further information on research design is available in the Nature Portfolio Reporting Summary linked to this article.

Results

Cellular and molecular landscape of healthy human knee at single-cell resolution

We used scRNA-seq to explore the cellular and molecular features of the human knee joint. This helps us understand how different tissues contribute to their normal functions. Healthy cartilage, meniscus, SynoFP, and SCB were combined and grouped together. We then analyzed cell identity using the H*umanPrimaryCellAtlas* database in *celldex* using *SingleR* R package (Fig. 2a; Figure. S1a, b). UMAP shows all the identified cell types, and Supplementary Data 1 shows the proportion of each cell type (Fig. 2a). The chondrocyte population was dominant and contributed to ~99.6% of the healthy cartilage samples, whereas the TSCs population contributed only ~0.4% of the total cell population (Fig. 2b; Figure. S1b). The chondrocyte population was also enriched in the meniscus, contributing ~85.3%, along with ~9.5% of TSCs and a small proportion of endothelial cells (EC) (~ 2.7%), smooth muscle cells (SMC) (~ 1.3%), fibroblasts (~ 0.5%), and immune cells (including ~0.7% macrophages). However, the proportion of chondrocytes was low in the SynoFP group (approximately 15%) and nearly absent in the SCB group (0.3%).

The TSCs pool was notably higher in SynoFP. This accounted for approximately 42.2% of the total cell population. The breakdown included ~15.7% ECs, ~13.1% macrophages, ~5% monocytes, ~5.4% SMCs, ~1.5% synovial fibroblasts, and a small number of other immune cells. In SCB, T cells make up about 48.9% and NK cells about 36.1%. Together, these cells accounted for nearly 85% of all the cells. Other immune cells included macrophages (2.8%), monocytes (2.7%), TSCs (1.7%), and others. Overall, these data suggest that chondrocytes are predominant in the cartilage and meniscus, TSCs largely reside in SynoFP and the meniscus, and SynoFP and SCB are the major reservoirs of immune cells in healthy human knees.

To identify signaling and communication, CellChat analysis was performed, which revealed active communication among all four tissues. The cartilage was the major sender and receiver of the signals, followed by the meniscus and SynoFP. SCB was mainly a receiver of signals from the remaining three tissues (Fig. 2c). Analysis of cell types showed that MSCs, fibroblasts, SMCs, chondrocytes, and TSCs were the major senders of the signals, whereas MSCs, macrophages, monocytes, dendritic cells (DCs), and T cells were the major receivers (Fig. 2d, e). Approximately 85 signaling pathways actively send and receive signals. The most active top 10 signaling pathways were COLLAGEN, MIF, MHC-I, MHC-II, FN1, CD99, LAMININ, APP, CypA, and CXCL (Fig. 2f, Figure. S1d).

Pseudotime trajectory analysis which determines the origin and terminal differentiation state of chondrocytes[26], was performed by extracting TSCs and chondrocytes from the total cell population (Fig. 2g). Using TSCs clusters as a root node, we performed an analysis and visualized them on UMAP (Fig. 2h). All four tissues contributed to the TSCs and chondrocyte populations; however, the contribution of SCB was negligible (Figure. S1e). Cluster 8 had the lowest Pseudotime since it mostly consists of TSCs and is considered a root node, whereas Cluster 5 and Cluster 0 had the highest Pseudotime, suggesting the terminally differentiated chondrocyte population, primarily residing in the cartilage (Fig. 2i; Fig. S1b, e).

Cellular and molecular landscape of the human knee during OA at single-cell resolution

To evaluate changes in cellular homeostasis during OA, samples were subjected to clustering and cell type identification (Fig. 3a; Figure. S2a, b). Supplementary Data 2 lists the proportion of each cell type. OA cartilage had more than ~99% chondrocyte population, ~0.1% TSCs, 0.4% macrophages, and 0.1% monocytes (Fig. 3b; Fig. S2c). In the OA meniscus, the population comprised approximately 82.6% chondrocytes, 6.8% TSCs, 3.9% macrophages, 2.8% ECs, 1.2% SMCs, 0.8% monocytes, and 0.3% fibroblasts. OA synovium contains ~37.5% chondrocytes and 16.4% TSCs. Interestingly, the synovium had a higher number of macrophages (~13.7%), fibroblasts (~7.7%), and monocytes (~1.8%), suggesting increased fibrosis and inflammation in knee OA. In SCB, NK cells (~32.6%) and T cells (~50.6%) contribute to ~83.2% of the total cell population, along with a small proportion of TSCs (~2%), macrophages (~1.3%), monocytes (~3.3%), chondrocytes (~1%), and other immune cells. Overall, the chondrocyte population significantly increased in the OA synovium. In contrast, the number of TSCs in the OA synovium and meniscus was reduced. Macrophage infiltration increases in the meniscus and synovium. Monocyte

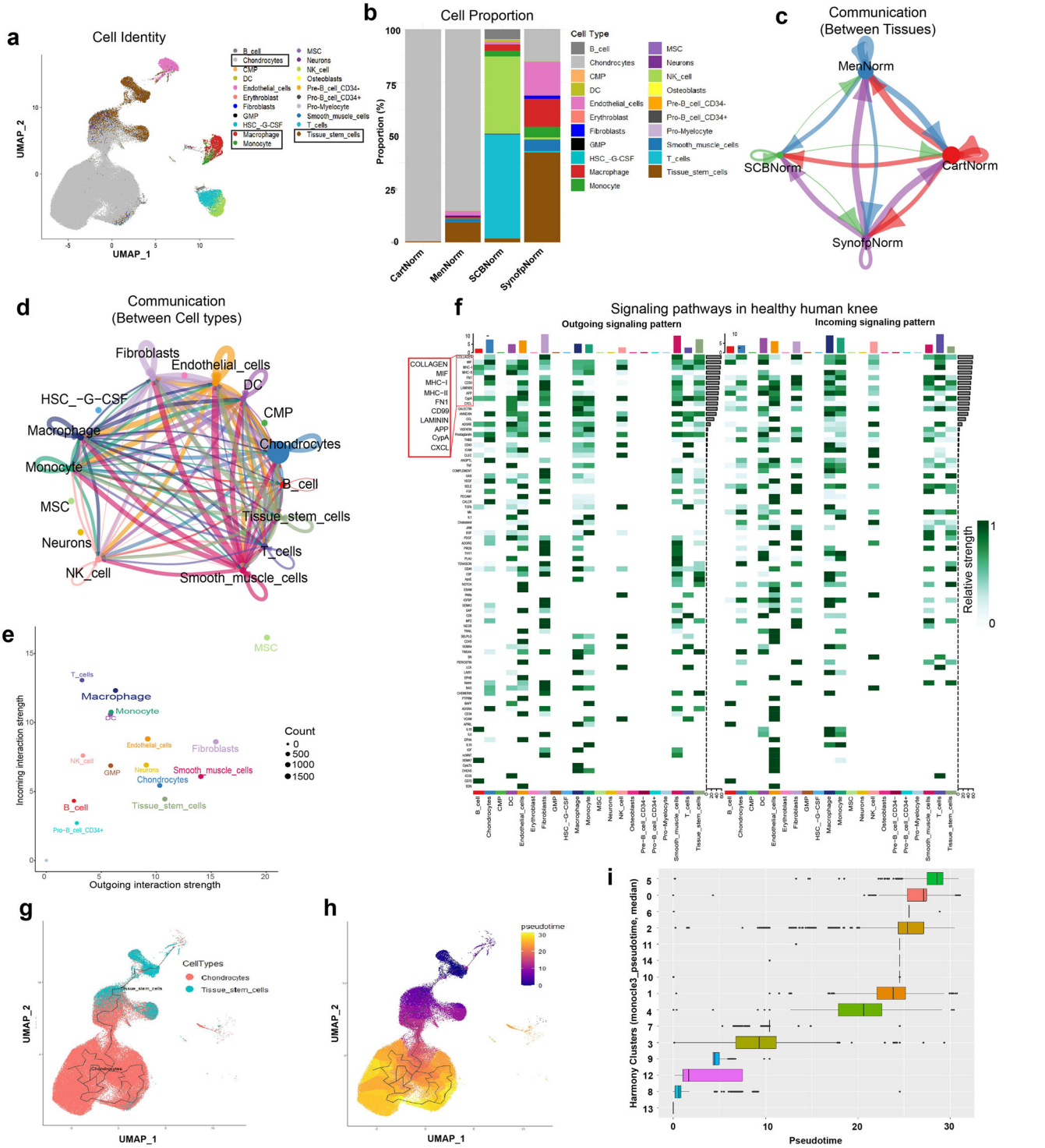

Fig. 2 | Cellular and molecular landscape of healthy human knees. a UMAP representation of total cell types in healthy human knee identified by SingleR. **b** Proportion of each cell type in a healthy human knee; here, the chondrocytes predominantly reside in cartilage and meniscus, TSCs in SynoFP and meniscus, and immune cells in SynoFP, subchondral bone, and meniscus. **c** Chord diagram showing communication between all four tissue types. **d** Chord diagram showing communications between different cell types. **e** Scatter plot showing outgoing and incoming interaction strength for different cell types; cell types with molecularly significant differences are shown in the broad letter. **f** Heatmap representation of active signaling pathways in the healthy human knee with outgoing and incoming signaling patterns; here, the top signaling pathways are highlighted in the red rectangle. **g** UMAP highlighted the location of chondrocytes and TSCs for pseudotime trajectory analysis. **h** UMAP visualization of pseudotime trajectory analysis; the root node was selected from the TSCs cluster. **i** Horizontal box plot showing pseudotime for individual harmony clusters.

infiltration was elevated, whereas ECs infiltration was reduced in the synovium.

CellChat analysis showed that OA cartilage was a major sender and receiver of signals, followed by the meniscus and synovium, whereas the SCB was mainly a receiver of signals from the remaining three tissues (Fig. 3c). Unlike in healthy tissues, the number of interactions increased between cartilage and SynoFP and meniscus and synoFP, suggesting active immune signaling during OA. Strong intercellular interactions were

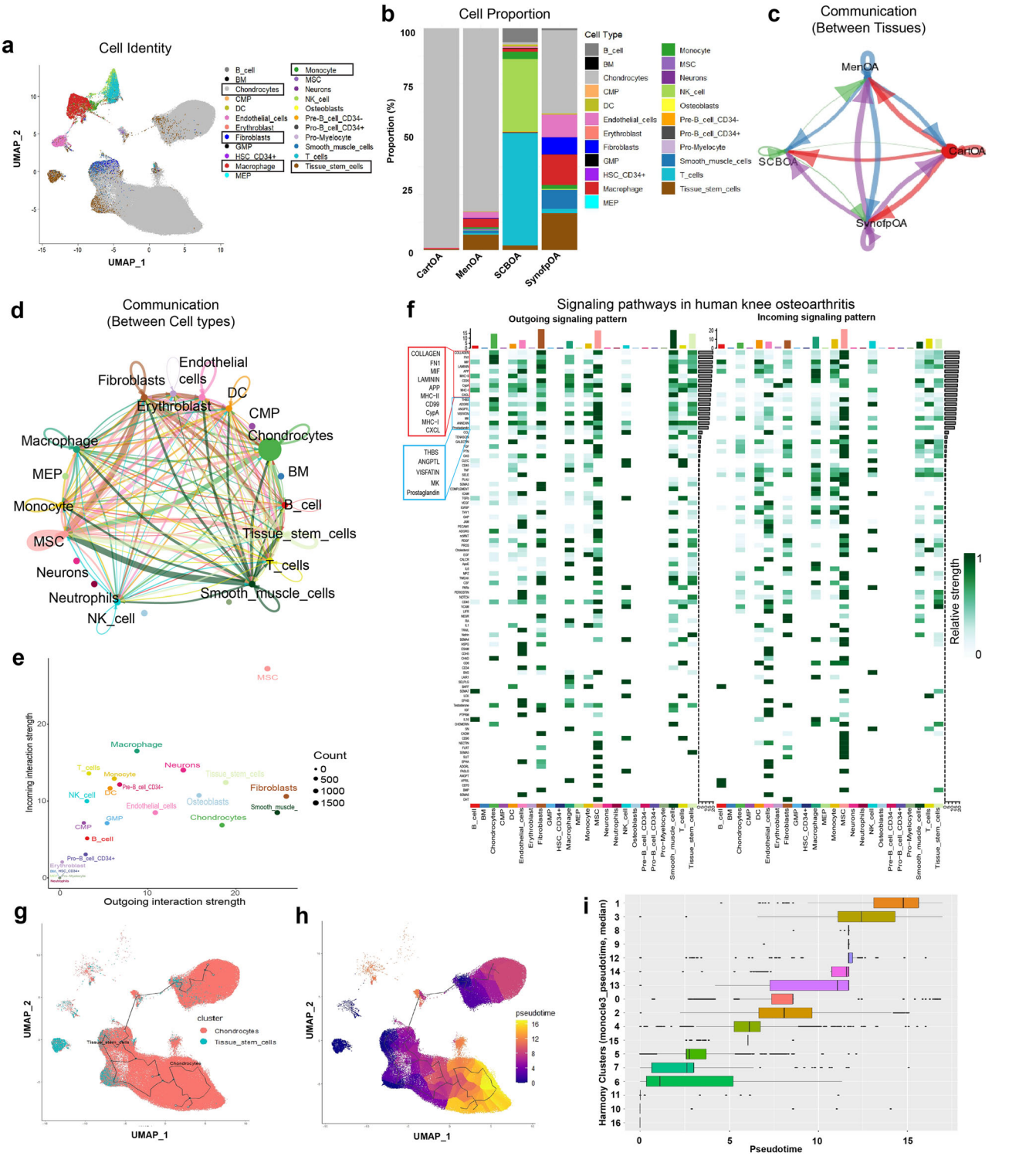

Fig. 3 | Cellular and molecular landscape during human knee OA. a UMAP representation of total cell types during OA condition identified by SingleR. **b** Proportion of each cell type in the human knee with OA; here, the chondrocytes predominantly resided in cartilage and meniscus, TSCs in SynoFP and meniscus, and immune cells in SynoFP, subchondral bone and meniscus. **c** Chord diagram showing communication between all four tissue types. **d** Chord diagram showing communications between different cell types. **e** Scatter plot showing outgoing and incoming interaction strength for different cell types; cell types with molecularly significant differences are shown in the broad letter. **f** Heatmap representation of active signaling pathways in the healthy human knee with outgoing and incoming signaling pattern; the top signaling pathways are highlighted in the red rectangle, whereas OA-specific active signaling pathways are highlighted with the blue rectangle. **g** UMAP highlighted the location of chondrocytes and TSCs for pseudotime trajectory analysis. **h** UMAP visualization of pseudotime trajectory analysis; here, the root node was selected from the TSCs cluster. **i** Horizontal box plot showing pseudotime for individual harmony clusters.

observed between cell types (Fig. 3d; Fig. S2d). MSCs, fibroblasts, SMCs, chondrocytes, TSCs, neurons, fibroblasts, and macrophages were the major senders of these signals, whereas MSCs, macrophages, neurons, and TSCs were major receivers (Fig. 3e). OA promotes intricate processes, such as cartilage degradation, inflammation, and pain, which are influenced by specific signaling pathways[50–55]. The top 10 most active signaling pathways in OA were COLLAGEN, FN1, MIF, LAMININ, APP, MHC-II, CD99, CypA, MHC-I, and CXCL (Fig. 3f). Additional pathways, such as prostaglandins, MK, VISFATIN, ANGPTL, and THBS, were highly active in OA (Fig. 3f; Fig. S2d).

Pseudotime trajectory analysis identified terminally differentiated chondrocytes increased in cartilage as well as meniscus since both these tissues contributed to the highest Pseudotime clusters 1 and 3 (Fig. 3g–i; Fig. S2e). Thus, the reduced TSCs population in meniscus and synovium OA compared to the healthy knee joint shows a transition to terminally differentiated chondrocytes, which contributes to fibrosis or osteogenic transition in OA. While these data reveal major cellular abnormalities in the synovium and meniscus during OA, they do not establish the synovium as the primary cause of OA. To understand the spatiotemporal roots of OA pathogenesis, in-depth investigation of different tissues and disease phases is required. Our findings do not indicate that synovial TSCs migrate into cartilage tissue. Rather, the observed continuity in the pseudotime trajectory implies a common transcriptional and presumably developmental program among the TSCs found in the synovium, meniscus, and cartilage. Instead of demonstrating direct migration events, this genetic or molecular linkage shows that these cells have a shared progenitor lineage or similar differentiation potential.

MMP13-producing detrimental chondrocytes and synovial fibroblasts were expanded in OA

To detect unique cellular and molecular OA-specific variations, healthy and OA knee scRNA-seq samples were integrated and subjected to harmony integration following standard Seurat processing (Figure. S3a). Cell type detection using singleR revealed variability in the population of major cell types, such as chondrocytes, TSCs, macrophages, and most importantly, expansion of synovial fibroblasts in OA (Fig. 4a, Fig. S3b, c). To correlate with the individual analyses described above, a stacked bar plot was generated, and the cell proportions in both sample types were compared (Figure. S3d). Clustering was performed at a resolution of 0.5 and generated nearly 27 cell clusters with clusters 3, 10, 18, 19, and 21 expanded, whereas major cluster 1 was depleted in the OA samples (Fig. 4d). All marker analyses were performed to determine the molecular identity of these clusters (Supplementary Data 3).

OA-depleted Cluster 1 expressed genes such as *CYTL1, CLEC3A, S100B*, and *FRZB*, which are effector chondrocyte (EC) markers[56] (Supplementary Data 3). These EC also produce *WISP3*[57], *CTGF*[58], *CYR61*[58], *GREM1*[59], and WIF1[60], which play roles in chondrocyte protection, angiogenesis, and ECM remodeling (Supplementary Data 3).

OA-specific chondrocyte cluster 3 (Fig. 4b), which is absent in healthy samples, contains specific detrimental chondrocytes (DCs) that promote cartilage/ECM degeneration, chondrocyte-to-osteoblast transition, and inflammation-related factors. DCs were enriched in *MMP13*[61], *TNFRSF11B* (osteoprotegerin)[62], *LCN2*[63,64], *MMP1*[65], *MMP3*[66], *ELF3*[67,68], *WNT7B*[60], and *NOS2*[69] (Fig. 4c) and are referred to as MMP13-producing DCs (MDCs). Next, we confirmed that MDCs primarily produce OA-specific markers (Fig. 4d; Fig. S3e, f). MDCs specifically produced *CCL20* and *LAMB3*, which are important factors for inflammatory pain and cartilage damage, respectively[70,71] (Fig. 4e).

Cluster 18 was exclusively present in OA samples and was molecularly aligned with the previously described pathogenic chondrocyte subpopulation owing to the higher expression of *POSTN* and *ZEB1*[28]. It highly expressed genes, such as *NELL1*[72,73], *LRRC15*[74], and *COL3A1*[75], which play a role in OA progression via osteogenesis, fibrosis, and ECM degeneration (Supplementary Data 3). Cluster 18 also expressed *RUNX2, ASPN*, and *OGN*, which promote mineralization and osteoblasts (Fig. 4f). Cluster 18 expressing genes showed negligible expression in the MDCs. Thus, cluster 18 and MDCs may contribute to the worsening of the disease pathology in human knee OA.

Cluster 10 showed slightly elevated levels of OA-expressing *CHI3L1, CHI3L2, MT1G, MT1H*, and *MT1E* regulatory chondrocyte markers (RegC)[28]. Cluster 19 comprised chondrocytes highly expressing IL10[76], *TM4SF1*[77], *CHADL*[78], *MIA*[79], *MT1G*[80], and *COL2A1*, which are associated with cartilage protection, matrix proteoglycan synthesis, and reversal of calcification and degeneration. Therefore, clusters 10 and 19 appear to expand because of a compensatory response to protect the knee joint from degenerative effects of OA.

Overall, *MMP13* expressing DCs and cluster 18 expressing factors may play a role in specific pathologies and mechanisms of OA development, whereas restoring cluster 1 and 19 factors may reverse OA. In addition, expansion of the fibroblast population may result in fibrosis in the synovial region, adding a layer to the pathophysiology of OA[81].

Synovium and meniscus are the primary residences for TSCs that are depleted in OA

The TSC population was significantly reduced in the SynoFP and meniscal groups. In the meniscus, the TSCs proportion decreased from ~9.5% to ~6.8%, and SynoFP from ~42.2% to ~16.4%, which can also be correlated with the expansion of the differentiated chondrocyte population in SynoFP (from ~15% to ~37.5%) during OA (Fig. 5a). For further analysis, we extracted TSCs from the total cell clusters and generated UMAP cells to visualize the reduced regenerative (chondrogenic factor production) and increased osteogenic TSCs in OA (Fig. 5b). As TSCs primarily reside in the meniscus and SynoFP, we generated UMAP to observe the different TSCs contributing to the different TSC subtypes (Fig. 5c). TSCs decreased by 36.45% in the meniscus and 37.77% in SynoFP compared with their respective healthy controls (Fig. 5d). We observed a reduction in the number of regenerative TSCs producing *CXCL12* (SDF1), *SOX9*, *ACAN, MCAM* (CD146), *PDGFRB, BMPR1B, ENG* (CD105/Endoglin), and *NGFR* (Fig. 5e and Fig. S4a, b). Previously identified chondroprogenitor and stem cell markers that express TSCs have also been affected[33–35]. These TSCs were SDF1 + [35], CD146 + [82], CD105 + [83–85] (Fig. 5f–h).

Interestingly, osteogenic TSCs expressing *ALCAM, NT5E* (CD73), *NGF*, and *BDNF* increased in OA. *NT5E* (CD73) is known to increase in OA (Fig. 5e)[86–88]. Comparative analysis of knee joint tissue compartments revealed that the meniscus and synovium are the primary residences of tissue stem cells, which are significantly depleted during OA, contributing to the worst pathological outcome.

Elevated levels of IL1B-IL6-NOS2-TNF and pain markers P2RX7-producing macrophages contribute to OA pathophysiology

We hypothesized that OA promotes the infiltration of proinflammatory cells, which initiates a vicious cycle of cytokine production, leading to knee joint inflammation and pain. Integration of healthy and OA samples revealed an expansion of the macrophage population in cluster 13 in OA samples (Fig. 4a, b). Within this macrophage population, we identified seven different subpopulations of macrophages at a resolution of 0.5 and labeled them as macrophage clusters MC1-MC7 (Fig. 6a). MC1 and MC2 were the largest clusters, with MC2 being largely expanded during OA, whereas MC3 and MC4 were exclusively present in OA samples (Fig. 6a).

To determine the levels of pro- and anti-inflammatory macrophages under healthy and OA conditions, we analyzed the levels of proinflammatory M1 (*CD86* and *TNF*) and anti-inflammatory M2 (*CD163* and *MRC1*)-type macrophages. We found that CD86- and TNF-producing macrophages were expanded in the OA samples, whereas CD163- and MRC1-expressing macrophages were significantly depleted (Fig. 6b). Feature plot analysis revealed that MC1 mostly expressed M2 macrophage markers whereas MC2 and MC3 mostly expressed M1 macrophage markers (Figure. S5a, b). Next, we analyzed the expression of the proinflammatory OA-causing markers *IL1B, IL6, TNF*, and *NOS2* within each macrophage cluster (Fig. 6c). Interestingly, *IL1B* and *TNF* were highly expressed in OA-

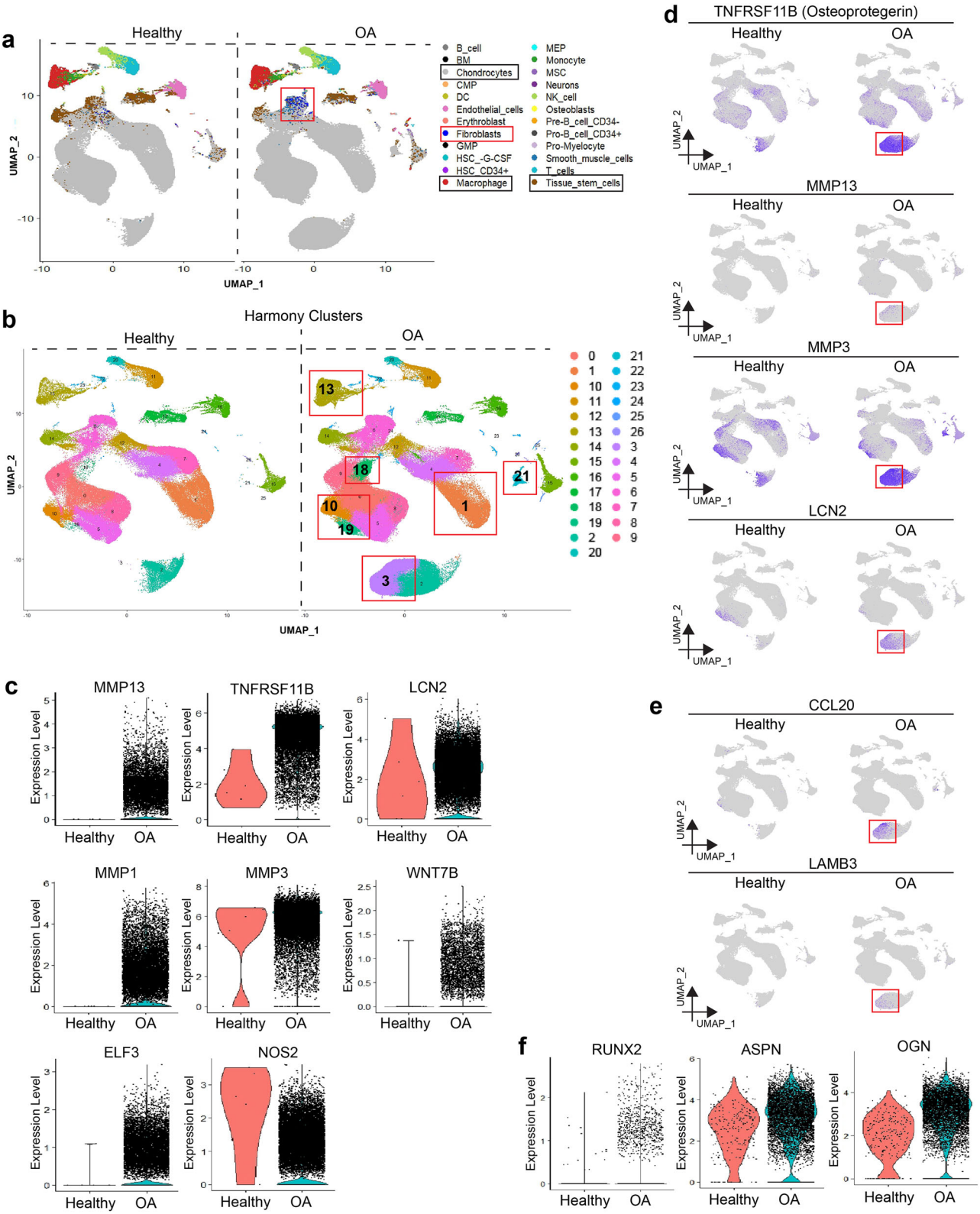

Fig. 4 | Integration of healthy and OA samples identified an OA-specific degenerative chondrocyte cluster. a UMAP representation of cell identity in Harmony integrated healthy and OA samples; rectangles show predominant cell types. **b** Total cell clusters ($n = 27$) across healthy and OA samples at 0.5 resolution; red boxes highlight the clusters variably present in OA samples. **c** Feature plots showing the total expression of top markers of Cluster 3 (MDCs) in both healthy and OA samples; red boxes highlight their expression levels (blue) in Cluster 3. **d** Violine plots showing upregulation of chondrocytes expressing OA-specific genes. **e** Feature plots showing the expression of *CCL20* and *LAMB3* in Cluster 3 (MDCs) of OA samples; red boxes highlight their expression levels (blue). **f** Violine plots showing chondrocytes expressing mineralization and osteogenic transition-related genes in Cluster 18.

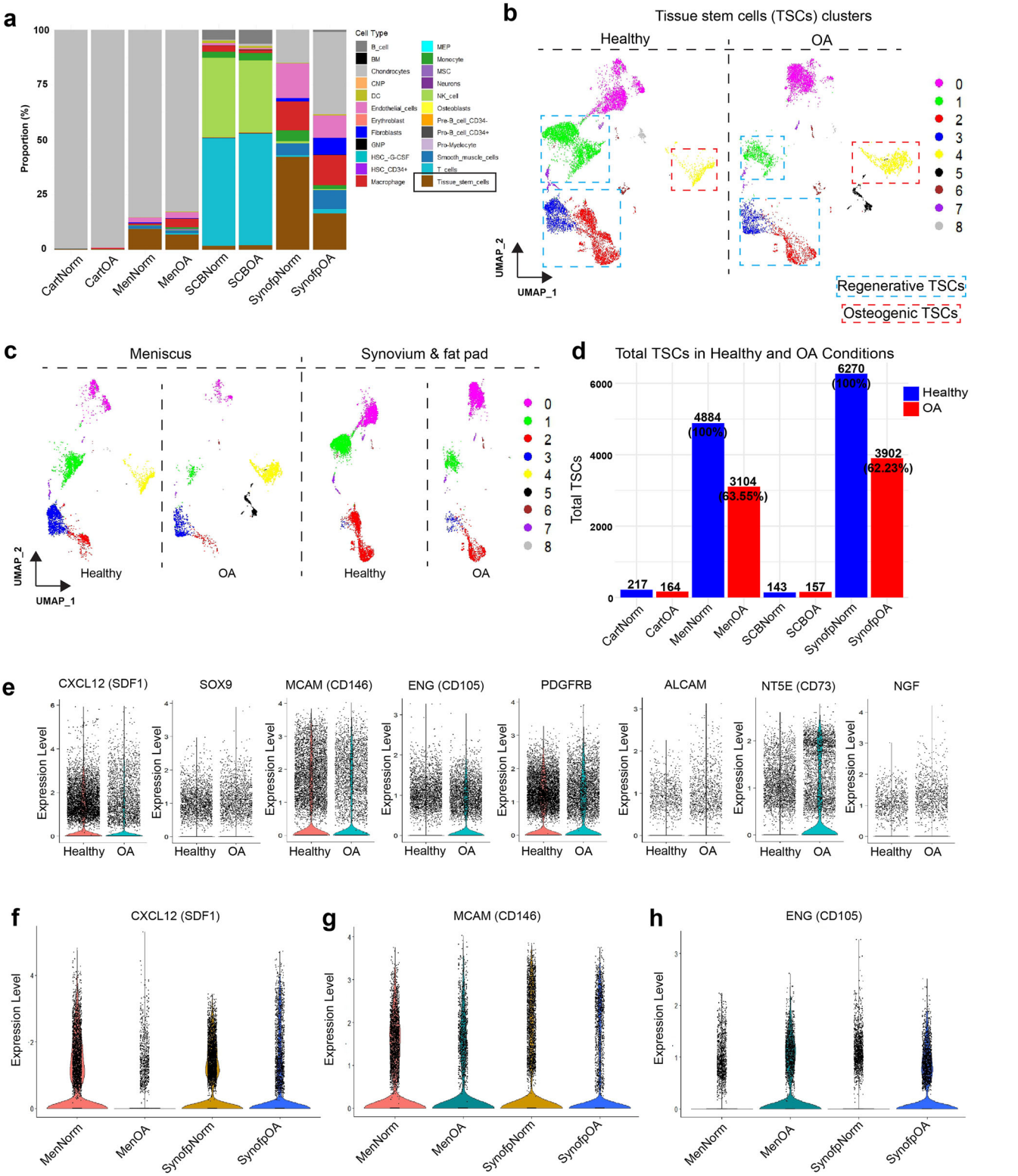

Fig. 5 | Synovium and meniscus are primary residences for tissue stem cells depleted due to OA. a Stacked bar plots show comparative cell type proportion in each tissue type during healthy and OA conditions; TSCs are shown in brown color and highlighted in a rectangle. **b** UMAP shows the drastic depletion of the TSCs pool in OA compared to the healthy samples. **c** Extraction and UMAP visualization of TSCs pool in meniscus and SynoFP during healthy and OA conditions. **d** Bar plots show levels of total TSCs in all four tissue types: CartNorm: Healthy cartilage, CartOA: OA cartilage, MenNorm: Healthy meniscus, MenOA: OA meniscus, SCBNorm: Healthy subchondral bone, SCBOA: OA subchondral bone, SynofpNorm: Healthy synovium & infrapatellar fat pad, SynofpOA: OA synovium & infrapatellar fat pad; (Blue: Healthy samples, Red: OA samples). **e** Violine plots show TSCs expressing chondroprogenitor and stem cell markers in healthy and OA conditions. **f–h***CXCL12* (SDF1), *MCAM* (CD146), and *ENG* (CD105, Endoglin) expressing TSCs from meniscus and SynoFP in healthy and OA conditions.

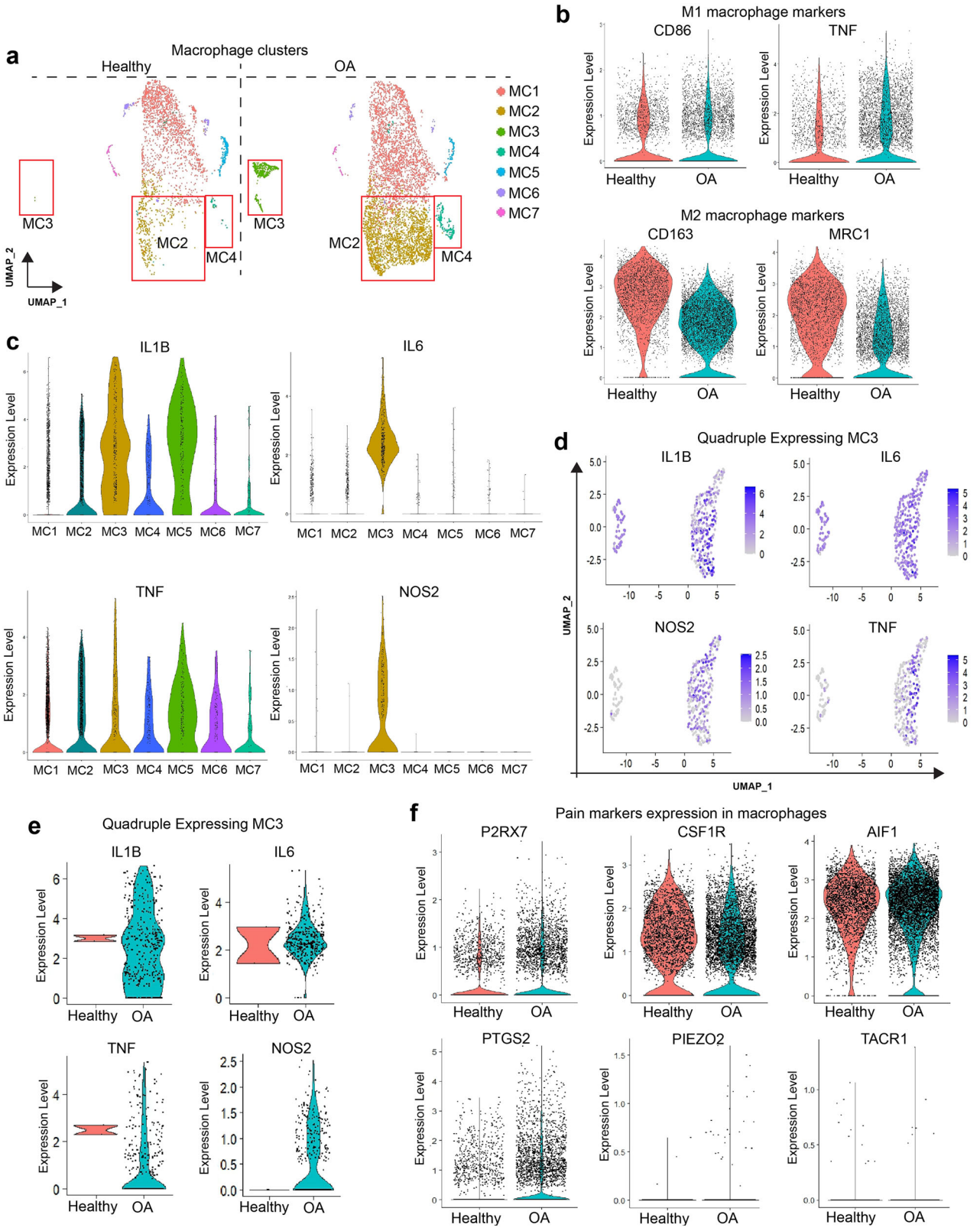

Fig. 6 | Increased levels of quadruple positive inflammation and pain-associated macrophages in OA. a Extraction and UMAP visualization of total macrophages in healthy and OA samples. The red boxes highlight macrophage subtypes enriched in OA samples: MC2, MC3, and MC4 (MC: Macrophage Cluster). **b** Visualization of M1 and M2 macrophages in healthy and OA samples, where we used *CD86* and *TNF* as classical M1 macrophage markers and *CD163* and *MRC1* as classical M2 macrophage markers. **c** Violine plots showing significant inflammatory markers expressing MCs, where MC3 stands out as a unique cluster expressing all four inflammatory markers (*IL1B, IL6, TNF*, and *NOS2*) (quadruple markers). **d**,**e** Feature plots and violin plots show MC3 expressing quadruple markers. **f** Violine plots showing higher enrichment of macrophages expressing classical pain markers in knee OA.

specific macrophages, MC2 and MC1, suggesting an *IL1B* + *TNF*+ inflammatory macrophage population, irrespective of their M1 and M2 status. These *IL1B*+ and *TNF*+ macrophages may serve as prognostic or diagnostic biomarkers of OA pathophysiology.

Notably, we discovered that MC3, a unique OA-specific macrophage cluster, was the only cluster that expressed all four proinflammatory genes: *IL1B, NOS2, IL6*, and *TNF* (Fig. 6c, Fig. S5a, e). Next, we extracted MC3 from the total macrophage clusters and confirmed the significantly upregulated expression of these genes in OA (Fig. 6d and e). These quadruple-positive macrophage subpopulations (*IL1B* + *IL6* + *NOS2* + *TNF* +) of inflammatory macrophages worsen the disease outcome in terms of joint inflammation and pain in patients with OA.

Finally, we analyzed the expression of classic pain marker genes in total macrophages to understand the association between OA macrophages and joint pain. As expected, *P2RX7*-, *CSF1R*-, *AIF1*-, and *PTGS2* (COX2)-producing macrophages were highly expanded in OA samples (Fig. 6f). However, two well-studied OA pain markers, *PIEZO2* and *TACR1*, were not expressed by macrophages. Thus, we conclude that clinical knee OA inflammation and pain arise due to the accumulation of dual- and quadruple-positive proinflammatory macrophages, which need to be functionally characterized in a large cohort of clinical samples in the future.

Intercellular crosstalk enhances joint inflammation and osteogenic transition in human knee OA

To evaluate the signaling events contributing to OA, we performed NicheNet analysis by considering macrophages as a receiver, whereas fibroblasts, tissue stem cells, and chondrocytes were the sender of signals. Here, we screened the top 30 ligands secreted by sender cell types that were received by macrophages (Fig. 7a). We found that synovial fibroblast-specific complement factor D (CFD) and LGALS3 (galectin-3) are important pro-inflammatory ligands because of their potential to bind macrophage-expressed receptors (Fig. 7b, c). CFD was among the top 20 ligands produced during OA (Fig. S6a). CFD, a serine protease, triggers an alternative complement pathway, resulting in the production of C3a and C5a. These molecules recruit and stimulate macrophages, enabling them to produce pro-inflammatory cytokines, such as TNFα and IL-1β[89–91]. Therefore, increased *CFD* expression may be correlated with macrophage-driven synovitis and cartilage matrix degradation. Similarly, *LGALS3* produced by synovial fibroblasts promotes macrophage activation and survival via galectin-3-mediated binding to glycosylated surface receptors, thereby enhancing *IL1B, TNFA, MMP1, MMP3*, and *MMP13* production[92,93]. Together, CFD and LGALS3 in fibroblasts create a pro-inflammatory microenvironment that perpetuates macrophage activation and OA progression.

TIMP1, a ligand secreted by chondrocytes (Fig. 7b), particularly MDCs (Fig. 7d), binds to the CD63/integrin β1 complex on the surface of macrophages (Fig. 7c, e). This activates intracellular signaling cascades such as PI3K/AKT and ERK/FAK, promoting cell survival and resistance to apoptosis[94]. This extended survival may be a factor in the accumulation of pro-inflammatory macrophages in the OA joint environment, which in turn attracts and stimulates additional immune cells.

We then switched TSCs as receivers, whereas fibroblasts, macrophages, and chondrocytes were the senders of the signals. The top 30 factors released by the sender, which were received by the TSCs, were screened (Fig. 7f). Interestingly, chondrocytes released ligands such as MELTF and BMP2, whereas fibroblasts released FBLN2, COL6A3, and LGALS3BP, which transition TSCs to osteogenic early osteogenic and quiescent states, eventually contributing to OA (Fig. 7g, h). In addition, MELTF and BMP2 were among the top 20 ligands produced by all OA cell types (Fig. S6b).

Fibroblast-released CSF1 may cause TSCs to transition into macrophages (Fig. 7g and h). Additionally, C1QB released by macrophages could induce the activation, differentiation, and migration of neural stem cells within the TSCs population and most likely contribute to the perception of OA pain[95,96] (Fig. 7g, h).

High TGF-β1 levels induce abnormal bone growth, poor bone quality, and disease severity, along with increased angiogenesis[97,98]. In several animal models of OA, degenerative changes in the SCB are reduced and articular cartilage degradation is decreased when TGF-β1 activity is inhibited[97]. To evaluate whether the SCB receives TGFB1 signals from the other three tissues, we performed NicheNet analysis, which focused on ligand receptor activity between the SCB and SynoFP/Meniscus/Cartilage. We found that cartilage produced the ligand TGFB1 (Fig. 7i), more specifically by MDCs (Fig. 7d), and was predicted to be received by SCB via the TGFBR1 receptor (Fig. 7j). Other highly produced ligands, such as GNAS by Meniscus, B2M, SERPING1, TIMP2 by SynoFP, and CD55 by cartilage could also elicit OA severity through aberrant activity of SCB; however, this requires further investigation. Taken together, these data suggest that SCB plays an active role in the development and progression of OA.

Synovium and meniscus are an epicenter for immune activity in human knee

To understand the effect of dual- and quadruple-positive proinflammatory macrophages and inflammatory changes in OA, we performed individual tissue-specific (i.e., Cartilage, Meniscus, SynoFP, and SCB) immune cell infiltration and gene expression analyses, and all marker analyses were performed (Supplementary Data 4). Gene analysis showed that *LEFTY2, WISP2, IL6, IGF1*, and *COL1A1* were abundantly expressed in the normal meniscus compared to the other three tissue types (Fig. 8a). In the OA meniscus, major histocompatibility complex (MHC) class I antigen genes *HLA.A, HLA.B*, and *HLA.C* were increased along with elevated expression of other key immune response genes, such as *WISP2, IL6*, or *CXCL6*, with a higher fold change (Fig. 8b). The normal synovium showed the expression of *CD163*, an immunosuppressive M2 type macrophage, which was absent in the OA synovium (Fig. 8c, d). Moreover, the OA synovium highly expresses pain and inflammatory genes such as *PI16, CCL14, CD248, C3*, and *CCL3L1* (Fig. 8d).

Next, we applied GSEA with tissue-specific markers and all-marker analysis. This helped us to evaluate the networks and pathways activated in OA. The OA cartilage had a higher enrichment of bone mineralization, cartilage development, ossification, and osteoblast differentiation, which are associated with OA pathology (Fig. 8e). OA synovium showed significant enrichment of activation of the immune response, adaptive immune response, antigen presentation via MHC class II, and activation of the complement pathway (Fig. 8f). Taken together, the expression of tissue-specific genes, inflammatory cells, and macrophages in the meniscus and synovium of the human knee significantly contributes to OA development and progression.

Discussion

Although OA is a whole joint disease, the contribution of tissue-specific cells to disease onset and transcriptional changes is unknown. An atlas was constructed by integrating single-cell RNA sequencing profiles of human knee cartilage, meniscus, synovium, and SCB. This revealed clear differences between healthy knees and those with OA. We found that TSCs and immune signaling are active during OA. Terminally differentiated chondrocytes in OA have a transcriptomic association with TSCs residing in the synovium and meniscus, which were identified using pseudotime trajectory analysis. Our findings highlight that synovium may be a hotspot for degenerative and regenerative events. TSCs, multi-tissue interactions, and inflammation may affect cartilage integrity.

TSCs primarily reside in the synovium, and regenerative TSCs are depleted in OA. This dynamic change reduced regeneration and increased degeneration. Regenerative TSCs[33–35] express markers such as *CXCL12* (SDF1), *SOX9, ACAN, MCAM* (CD146), *PDGFRB, BMPR1B, ENG* (CD105/Endoglin), and *NGFR*. SDF1-expressing TSCs are explicitly depleted in the meniscus, and studies have shown that SDF1 is required for chondroprogenitor cell migration during post-injury tissue repair in the meniscus[35]. MCAM+ (CD146 +) stem cells have previously shown a more significant migration potential towards degenerated intervertebral disks[82].

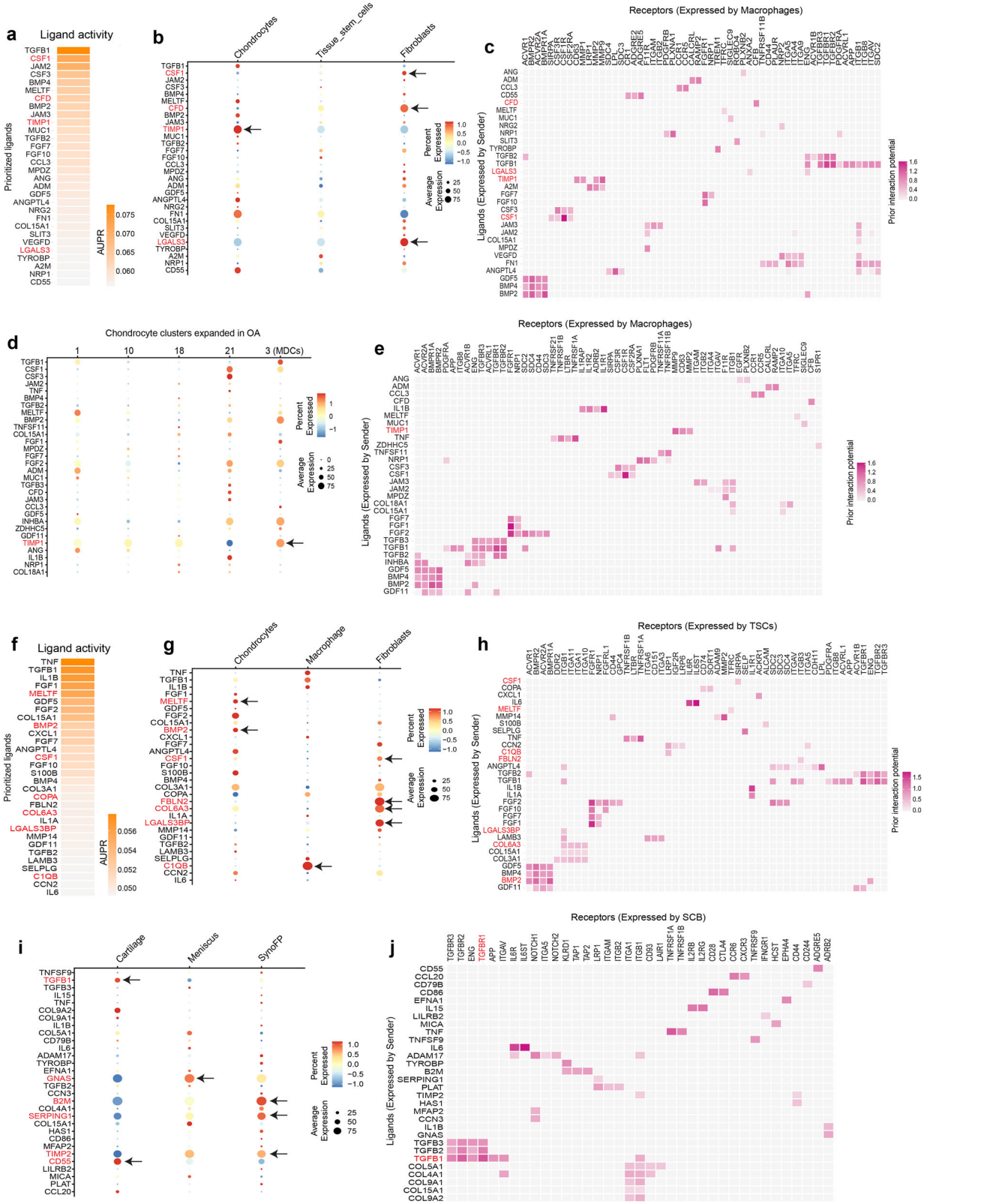

CD105 promotes chondrogenesis in synovium-derived MSCs[83,84]. Osteogenic TSCs expressing *ALCAM, NT5E* (CD73), *NGF*, and *BDNF* expanded in OA. ALCAM+ cells can differentiate into osteoblasts, adipocytes, chondrocytes, and stromal cells, which support osteoclastogenesis, hematopoiesis, and angiogenesis[99]. NT5E is a marker of resting chondrocytes[88] and is up-regulated in OA[86–88]. In addition, expanded fibroblasts in the OA synovium may contribute to fibrosis in knees with OA.

OA-specific MDCs are enriched with degradative factors such as LCN2[63], TNFRSF11B[62], MMP1, MMP3, MMP13, NOS2, WNT7B[60], and ELF3[67,68]. They play a significant role in extracellular matrix destruction,

Fig. 7 | Intercellular crosstalk enhances joint inflammation and osteogenic transition during OA. a Ligand activity plot for top 30 ligands produced by senders (chondrocytes, TSCs, and fibroblasts), whose receptors were expressed by macrophage. **b** Bubble plot shows the expression of ligands in individual sender. Arrow indicates the significant genes described in the results section. **c** Heatmap shows the interaction potential of ligand produced by senders and receptors expressed by macrophage. **d** Expression of ligands produced by OA specific chondrocyte clusters, which interact with the receptors expressed by macrophage. Arrow indicates significant gene *TIMP1* specifically expressed by MDCs. **e** Interaction potential of top 30 ligands produced by OA specific chondrocyte clusters with receptors expressed by macrophage. Here, *TIMP1* from MDCs shows interaction potential with CD63 of macrophage. **f** Ligand activity plot for top 30 ligands produced by senders (chondrocytes, macrophage, and fibroblasts), whose receptors were expressed by TSCs. **g** Expression levels of ligands in individual sender. Arrow indicates the significant genes described in the results section. **h** Interaction potential of ligand produced by senders and receptors expressed by TSCs. **i** Expression levels of ligands in individual sender tissue. Arrow indicates the significant genes described in the results section. **j** Interaction potential of ligand produced by senders and receptors expressed by SCB.

bone remodeling, and cartilage degradation. OA-specific cluster 18 was enriched with RUNX2[73], ASPN, and OGN, which are markers of mineralization and osteoblast characteristics[62] that contribute to stiffness. OA-specific MDCs were enriched in CCL20 and other markers associated with inflammation and pain. In the presence of CCL20, cartilage released more MMP-1, MMP-13, PGE2, GAG fragments, and IL-6, whereas collagen type II mRNA expression was inhibited[70].

Many factors such as long-term injury and mechanical changes can cause OA. However, our analysis revealed a significant increase in inflammation- and pain-related macrophages in patients with OA. A unique dual positive (IL1B and TNF) and quadruple positive (IL1B, TNF, IL6, and NOS2) macrophage subpopulation could play a significant role in promoting inflammatory changes are not known yet. Traditionally, macrophage classification in OA has been based on the M1/M2 paradigm, in which M1 macrophages are pro-inflammatory and M2 macrophages are anti-inflammatory. However, this binary framework may not adequately represent the complexity of macrophage phenotypes in OA patients. It has been anticipated that macrophage polarization can go beyond the typical binary state[100]. Our discovery of a quadruple-positive macrophage subpopulation, which is defined by the co-expression of markers IL1B, IL6, TNF, and NOS2, represents an important advancement beyond the traditional M1/M2 categorization. These cells have a particular inflammatory gene expression profile and are almost entirely absent in healthy non-OA knee joints, indicating disease-specific traits. Their exclusive emergence in the OA environment suggests a potentially important role in disease pathophysiology, making them previously unidentified contributors to OA progression. Therefore, this finding not only broadens our understanding of macrophage heterogeneity in OA but also opens new avenues for targeted therapeutic intervention.

Additionally, the OA meniscus highly expressed well-characterized immune response genes including *HLA.A, HLA.B, HLA.C, WISP2, IL6*, and *CXCL6*. The OA synovium also expresses pain and inflammatory genes, such as *PI16, CCL14, CD248, C3*, and *CCL3L1*. The OA synovium also showed higher enrichment of activation of the immune response, antigen presentation, and complement activation compared to the cartilage, meniscus, and SCB during OA.

The structural integrity and homeostasis of the ECM are maintained in healthy joints through signaling pathways, such as COLLAGEN, FN1, LAMININ, and THBS, which support cartilage resilience and joint lubrication. However, in OA, dysregulation of these pathways leads to matrix breakdown and chondrocyte apoptosis, which accelerates cartilage degradation[101–104]. The MHC-I and MHC-II pathways, which are normally associated with immune surveillance and tolerance, require further investigation in the setting of OA because of abnormal antigen presentation and persistent immunological activation. MIF and CXCL chemokines, which assist in controlling immune cell trafficking in healthy tissues, may become pro-inflammatory in OA, activating synovial macrophages and inducing cartilage catabolism[105–108]. It has been previously demonstrated that CD99 contributes to leukocyte infiltration during inflammatory events and that blocking CD99 reduces inflammation[109]. However, its role in OA requires further evaluation. CypA and VISFATIN, involved in redox balance and metabolic regulation under physiological conditions, promote oxidative stress and inflammation in OA and correlate with cartilage degradation biomarkers[52,110,111]. ANGPTL and MK (midkine), which are involved in tissue repair, become pathogenic by stimulating synovial angiogenesis and inflammation[112–115]. Finally, prostaglandin signaling is essential for normal knee function, and imbalance in prostaglandin production or signaling can lead to inflammatory OA[50]. Thus, when these physiological pathways that promote joint function are persistently active or unbalanced, they become the pathological drivers of OA.

The limitation of this study is that, although we generated the first scRNA-seq atlas to identify key genes, cell types, and therapeutic understanding of OA pathogenesis, the inclusion of a state-specific and progressive OA-grade multi-tissue analysis will provide detailed information on OA progression and severity. OA disproportionately affects underserved populations[116,117] and females. The detailed temporal and spatial appearance of RNA from the time of inciting injury through the initiation and progression of OA pathophysiology, its proteomics profile, and actual tissue changes need to be determined. Future studies should involve well-controlled clinical cohorts with large age- and sex-matched cohorts of samples, and standardized tissue extraction procedures. The discovery of quadruple-positive macrophages in this study is intriguing. However, in vitro and in vivo validation is required to validate their potential as predictive or diagnostic biomarkers of knee OA. While our findings indicate significant cellular abnormalities in the synovium and meniscus during OA, they do not establish the synovium as the primary etiology of OA. Transcriptional changes identified in specific cell types may be reactive to the OA microenvironment, such as inflammation or mechanical stress, rather than initiating processes. Nonetheless, the probability of initiating events cannot be ruled out, and will require experimental validation in the future. Moreover, co-culture experiments, ligand-receptor blocking studies, and experimental validation of TSC subtypes would provide more mechanistic insights into communication events between macrophages, MDCs, synovial fibroblasts, and TSCs during OA progression.

In conclusion, the synovium and meniscus are the most damaged compartments, and synovium regeneration could have potential therapeutic opportunities considering highly dysregulated homeostasis. Atala et. al. showed that the synovial environment causes cartilage deterioration and regeneration[118]. OA pain may be a consequence of resident TSCs depletion and proinflammatory changes in the synovium and meniscus. Moreover, dual- and quadruple-positive macrophages could serve as prognostic markers for identifying pre- and post-treatment OA severity. The transcriptional changes observed in specific cell populations may represent reactive responses to the OA microenvironment, such as inflammation or mechanical stress, rather than the initiation of events. Nonetheless, the possibility of initiating events cannot be ruled out and requires experimental validation in the future. Our findings also demonstrate that SCB plays an active role in OA. We found that TGFB1, which is mostly produced by cartilage cells, specifically MDCs, can signal SCB via the TGFBR1 receptor, indicating a potentially essential mechanism in disease progression. Other signals from the meniscus and synovial tissues may potentially influence SCB behavior and contribute to OA; however, further research is required to completely understand their impact.

As there are no FDA-approved drugs, our study suggests that future clinical trials should focus on synovium and meniscus regeneration. This is important for the design of OA disease-modifying drugs. Our analysis also emphasized the heterogeneity within the meniscus and bone compartments, revealing distinct cellular niches that may influence disease

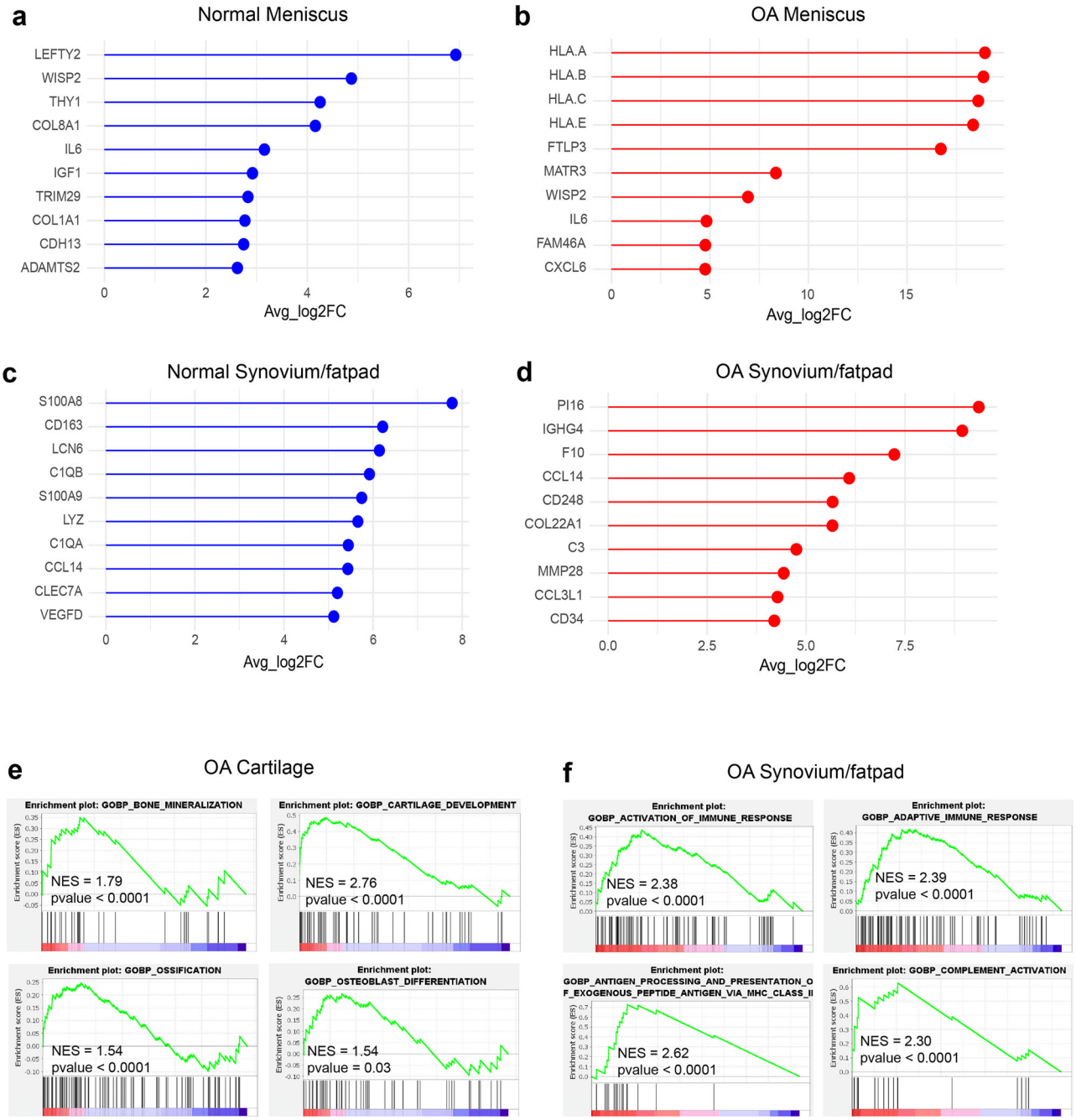

Fig. 8 | Meniscus and synovium are hubs for inflammatory immune activity during knee OA. a The expression of top marker genes expressed specifically in normal meniscus compared to other knee tissues in normal condition. Adjusted p value for the genes is below 0.0001. **b** The expression of top marker genes, specifically immune response genes, expressed highly in OA meniscus compared to other knee tissues in OA condition. Adjusted p value for the genes is below 0.0001. **c** The expression of top marker genes expressed specifically in normal synovium & fatpad compared to other knee tissues in normal condition. Adjusted p value for the genes is below 0.0001. **d** The expression of top marker genes, specifically pain and inflammation genes, expressed highly in OA synovium & fatpad compared to other knee tissues in OA condition. Adjusted p value for the genes is below 0.0001. **e** GSEA shows enrichment of gene sets related to cartilage damage in the OA cartilage. **f** Higher enrichment of immune response, antigen presentation, and complement activation in the OA synovium & fatpad. NES: Normalized Enrichment Score.

outcomes. Understanding the role of these niches in OA pathogenesis could lead to more targeted and effective treatment.

This atlas is a key resource of the scientific community. It offers new insights into cellular and molecular heterogeneity during healthy knee joint homeostasis and OA. In addition, it opens new possibilities for the development of targeted therapies to stop or reverse disease progression. Future studies should expand these findings. It is necessary to explore the complex cell activity in the OA joint. In addition, these insights should lead to clinical use.

Data availability

The human knee OA single-cell RNA-seq data used in this study are publicly available under the following accession ID: cartilage (GSE220243, GSE169454, and GSE255460); meniscus (GSE220243); synovium and IPFP (GSE216651); and SCB (GSE196678).

Received: 23 April 2025; Accepted: 24 July 2025;
Published online: 02 August 2025

References

1. Long, H. et al. Prevalence trends of site-specific osteoarthritis from 1990 to 2019: findings from the global burden of disease study 2019. *Arthritis Rheumatol.* **74**, 1172–1183 (2022).
2. Alshenibr, W. et al. Anabolic role of lysyl oxidase like-2 in cartilage of knee and temporomandibular joints with osteoarthritis. *Arthritis Res Ther.* **19**, 179 (2017).
3. Tashkandi, M. et al. Lysyl oxidase-like 2 protects against progressive and aging related knee joint osteoarthritis in mice. *Int J. Mol. Sci.* **20**, 4798 (2019).
4. Tashkandi, M. M. et al. LOXL2 promotes aggrecan and gender-specific anabolic differences to TMJ cartilage. *Sci. Rep.* **10**, 20179 (2020).
5. Arokoski, J., Kiviranta, I., Jurvelin, J., Tammi, M. & Helminen, H. J. Long-distance running causes site-dependent decrease of cartilage glycosaminoglycan content in the knee joints of beagle dogs. *Arthritis Rheum.* **36**, 1451–1459 (1993).
6. McDevitt, C. A. & Muir, H. Biochemical changes in the cartilage of the knee in experimental and natural osteoarthritis in the dog. *J. Bone Jt. Surg. Br.* **58**, 94–101 (1976).
7. Hoch, D. H., Grodzinsky, A. J., Koob, T. J., Albert, M. L. & Eyre, D. R. Early changes in material properties of rabbit articular cartilage after meniscectomy. *J. Orthop. Res* **1**, 4–12 (1983).
8. Tiderius, C. J., Olsson, L. E., Nyquist, F. & Dahlberg, L. Cartilage glycosaminoglycan loss in the acute phase after an anterior cruciate ligament injury: delayed gadolinium-enhanced magnetic resonance imaging of cartilage and synovial fluid analysis. *Arthritis Rheum.* **52**, 120–127 (2005).
9. Arokoski, J., Jurvelin, J., Kiviranta, I., Tammi, M. & Helminen, H. J. Softening of the lateral condyle articular cartilage in the canine knee joint after long distance (up to 40 km/day) running training lasting one year. *Int J. Sports Med* **15**, 254–260 (1994).
10. Setton, L. A., Elliott, D. M. & Mow, V. C. Altered mechanics of cartilage with osteoarthritis: human osteoarthritis and an experimental model of joint degeneration. *Osteoarthr. Cartil.* **7**, 2–14 (1999).
11. Stolz, M. et al. Early detection of aging cartilage and osteoarthritis in mice and patient samples using atomic force microscopy. *Nat. Nanotechnol.* **4**, 186–192 (2009).
12. Garnero, P. et al. Cross sectional evaluation of biochemical markers of bone, cartilage, and synovial tissue metabolism in patients with knee osteoarthritis: relations with disease activity and joint damage. *Ann. Rheum. Dis.* **60**, 619–626 (2001).
13. Aigner, T. et al. Large-scale gene expression profiling reveals major pathogenetic pathways of cartilage degeneration in osteoarthritis. *Arthritis Rheum.* **54**, 3533–3544 (2006).
14. Oungoulian, S. R. et al. Articular cartilage wear characterization with a particle sizing and counting analyzer. *J. Biomech. Eng.* **135**, 024501 (2013).
15. Workman, J., Thambyah, A. & Broom, N. The influence of early degenerative changes on the vulnerability of articular cartilage to impact-induced injury. *Clin. Biomech.* **43**, 40–49 (2017).
16. Steinmeyer, J., Knue, S., Raiss, R. X. & Pelzer, I. Effects of intermittently applied cyclic loading on proteoglycan metabolism and swelling behaviour of articular cartilage explants. *Osteoarthr. Cartil.* **7**, 155–164 (1999).
17. Hossain, M. J. et al. Anisotropic properties of articular cartilage in an accelerated in vitro wear test. *J. Mech. Behav. Biomed. Mater.* **109**, 103834 (2020).
18. Santos, S., Emery, N., Neu, C. P. & Pierce, D. M. Propagation of microcracks in collagen networks of cartilage under mechanical loads. *Osteoarthr. Cartil.* **27**, 1392–1402 (2019).
19. McNulty, A. L., Rothfusz, N. E., Leddy, H. A. & Guilak, F. Synovial fluid concentrations and relative potency of interleukin-1 alpha and beta in cartilage and meniscus degradation. *J. Orthop. Res.* **31**, 1039–1045 (2013).
20. Berg, W. B., van den, Loo, F. A., van de, Zwarts, W. A. & Otterness, I. G. Effects of murine recombinant interleukin 1 on intact homologous articular cartilage: a quantitative and autoradiographic study. *Ann. Rheum. Dis.* **47**, 855–863 (1988).
21. Fam, H., Bryant, J. T. & Kontopoulou, M. Rheological properties of synovial fluids. *Biorheology* **44**, 59–74 (2007).
22. Bonnevie, E. D. & Bonassar, L. J. A century of cartilage tribology research is informing lubrication therapies. *J. Biomech. Eng.* **142**, 031004 (2020).
23. Lin, W. & Klein, J. Recent progress in cartilage lubrication. *Adv. Mater.* **33**, 2005513 (2021).
24. Brophy, R. H. et al. Articular cartilage and meniscus predictors of patient-reported outcomes 10 years after anterior cruciate ligament reconstruction: a multicenter cohort study. *Am. J. Sports Med.* **49**, 2878–2888 (2021).
25. Sukopp, M. et al. Influence of menisci on tibiofemoral contact mechanics in human knees: a systematic review. *Front. Bioeng. Biotechnol.* **9**, 765596 (2021).
26. Katz, J. N., Arant, K. R. & Loeser, R. F. Diagnosis and treatment of hip and knee osteoarthritis: a review. *JAMA* **325**, 568–578 (2021).
27. Latourte, A., Kloppenburg, M. & Richette, P. Emerging pharmaceutical therapies for osteoarthritis. *Nat. Rev. Rheumatol.* **16**, 673–688 (2020).
28. Swahn, H. et al. Senescent cell population with ZEB1 transcription factor as its main regulator promotes osteoarthritis in cartilage and meniscus. *Ann. Rheum. Dis.* **82**, 403–415 (2023).
29. Tang, S. et al. Single-cell atlas of human infrapatellar fat pad and synovium implicates APOE signaling in osteoarthritis pathology. *Sci. Transl. Med* **16**, eadf4590 (2024).
30. Hu, Y. et al. Single-cell RNA-sequencing analysis reveals the molecular mechanism of subchondral bone cell heterogeneity in the development of osteoarthritis. *RMD Open* **8**, e002314 (2022).
31. Loeffler, M. & Roeder, I. Tissue stem cells: definition, plasticity, heterogeneity, self-organization and models-a conceptual approach. *Cells Tissues Organs* **171**, 8–26 (2002).
32. Fuchs, E. & Blau, H. M. Tissue stem cells: architects of their niches. *Cell Stem Cell* **27**, 532–556 (2020).
33. Dicks, A. et al. Prospective isolation of chondroprogenitors from human iPSCs based on cell surface markers identified using a CRISPR-Cas9-generated reporter. *Stem Cell Res. Ther.* **11**, 66 (2020).
34. Wu, C.-L. et al. Single cell transcriptomic analysis of human pluripotent stem cell chondrogenesis. *Nat. Commun.* **12**, 362 (2021).
35. Jayasuriya, C. T. et al. Human cartilage-derived progenitors resist terminal differentiation and require CXCR4 activation to successfully bridge meniscus tissue tears. *Stem Cells* **37**, 102–114 (2019).
36. Chen, H. et al. Molecular mechanisms of chondrocyte proliferation and differentiation. *Front. Cell Dev. Biol.* **9**, 664168 (2021).
37. Zha, K. et al. Heterogeneity of mesenchymal stem cells in cartilage regeneration: from characterization to application. *NPJ Regen. Med.* **6**, 14 (2021).
38. Fu, W. et al. 14-3-3 epsilon is an intracellular component of TNFR2 receptor complex and its activation protects against osteoarthritis. *Ann. Rheum. Dis.* **80**, 1615–1627 (2021).
39. Fan, Y. et al. Unveiling inflammatory and prehypertrophic cell populations as key contributors to knee cartilage degeneration in osteoarthritis using multi-omics data integration. *Ann. Rheum. Dis.* **83**, 926–944 (2024).
40. Jin, S., Plikus, M. V. & Nie, Q. CellChat for systematic analysis of cell-cell communication from single-cell transcriptomics. *Nat. Protoc.* **20**, 180–219 (2025).
41. Butler, A., Hoffman, P., Smibert, P., Papalexi, E. & Satija, R. Integrating single-cell transcriptomic data across different

conditions, technologies, and species. *Nat. Biotechnol.* **36**, 411–420 (2018).
42. McGinnis, C. S., Murrow, L. M. & Gartner, Z. J. DoubletFinder: doublet detection in single-cell RNA sequencing data using artificial nearest neighbors. *Cell Syst.* **8**, 329–337.e4 (2019).
43. Korsunsky, I. et al. Fast, sensitive and accurate integration of single-cell data with Harmony. *Nat. Methods* **16**, 1289–1296 (2019).
44. Hao, Y. et al. Dictionary learning for integrative, multimodal and scalable single-cell analysis. *Nat. Biotechnol.* **42**, 293–304 (2024).
45. Aran, D. et al. Reference-based analysis of lung single-cell sequencing reveals a transitional profibrotic macrophage. *Nat. Immunol.* **20**, 163–172 (2019).
46. Mabbott, N. A., Baillie, J. K., Brown, H., Freeman, T. C. & Hume, D. A. An expression atlas of human primary cells: inference of gene function from coexpression networks. *BMC Genomics* **14**, 632 (2013).
47. Jin, S. et al. Inference and analysis of cell-cell communication using CellChat. *Nat. Commun.* **12**, 1088 (2021).
48. Trapnell, C. et al. The dynamics and regulators of cell fate decisions are revealed by pseudotemporal ordering of single cells. *Nat. Biotechnol.* **32**, 381–386 (2014).
49. Browaeys, R., Saelens, W. & Saeys, Y. NicheNet: modeling intercellular communication by linking ligands to target genes. *Nat. Methods* **17**, 159–162 (2020).
50. Yang, D., Xu, K., Xu, X. & Xu, P. Revisiting prostaglandin E2: a promising therapeutic target for osteoarthritis. *Clin. Immunol.* **260**, 109904 (2024).
51. Deng, Q. et al. Midkine promotes articular chondrocyte proliferation through the MK-LRP1-nucleolin signaling pathway. *Cell Signal* **65**, 109423 (2020).
52. Franco-Trepat, E. et al. Visfatin connection: present and future in osteoarthritis and osteoporosis. *J. Clin. Med.* **8**, 1178 (2019).
53. Okada, T. et al. Synoviocyte-derived angiopoietin-like protein 2 contributes to synovial chronic inflammation in rheumatoid arthritis. *Am. J. Pathol.* **176**, 2309–2319 (2010).
54. Jia, C. et al. Silencing of angiopoietin-like protein 4 (Angptl4) decreases inflammation, extracellular matrix degradation, and apoptosis in osteoarthritis via the sirtuin 1/NF-κB pathway. *Oxid. Med. Cell Longev.* **2022**, 1135827 (2022).
55. Maumus, M. et al. Thrombospondin-1 partly mediates the cartilage protective effect of adipose-derived mesenchymal stem cells in osteoarthritis. *Front. Immunol.* **8**, 1638 (2017).
56. Ji, Q. et al. Single-cell RNA-seq analysis reveals the progression of human osteoarthritis. *Ann. Rheum. Dis.* **78**, 100–110 (2019).
57. Sen, M., Cheng, Y.-H., Goldring, M. B., Lotz, M. K. & Carson, D. A. WISP3-dependent regulation of type II collagen and aggrecan production in chondrocytes. *Arthritis Rheum.* **50**, 488–497 (2004).
58. Ungvari, Z. et al. Connective tissue growth factor (CTGF) in age-related vascular pathologies. *Geroscience* **39**, 491–498 (2017).
59. Ng, J. Q. et al. Loss of grem1-lineage chondrogenic progenitor cells causes osteoarthritis. *Nat. Commun.* **14**, 6909 (2023).
60. Cheng, J., Li, M. & Bai, R. The Wnt signaling cascade in the pathogenesis of osteoarthritis and related promising treatment strategies. *Front. Physiol.* **13**, 954454 (2022).
61. Hu, Q. & Ecker, M. Overview of MMP-13 as a promising target for the treatment of osteoarthritis. *Int J. Mol. Sci.* **22**, 1742 (2021).
62. Rodríguez Ruiz, A. et al. The role of TNFRSF11B in development of osteoarthritic cartilage. *Rheumatology***61**, 856–864 (2022).
63. Jaberi, S. A. et al. Lipocalin-2: Structure, function, distribution and role in metabolic disorders. *Biomed. Pharmacother.* **142**, 112002 (2021).
64. Villalvilla, A. et al. The adipokine lipocalin-2 in the context of the osteoarthritic osteochondral junction. *Sci. Rep.* **6**, 29243 (2016).
65. Wang, M., Zhou, Y., Huang, W., Zeng, Y. & Li, X. Association between matrix metalloproteinase-1 (MMP-1) protein level and the risk of rheumatoid arthritis and osteoarthritis: a meta-analysis. *Braz. J. Med Biol. Res.* **54**, e10366 (2020).
66. Sulastri, D. et al. Risk factor of elevated matrix metalloproteinase-3 gene expression in synovial fluid in knee osteoarthritis women. *PLoS One* **18**, e0283831 (2023).
67. Wondimu, E. B. et al. Elf3 contributes to cartilage degradation in vivo in a surgical model of post-traumatic osteoarthritis. *Sci. Rep.* **8**, 6438 (2018).
68. Otero, M. et al. ELF3 modulates type II collagen gene (COL2A1) transcription in chondrocytes by inhibiting SOX9-CBP/p300-driven histone acetyltransferase activity. *Connect Tissue Res.* **58**, 15–26 (2017).
69. Shen, P. et al. NOS inhibition reverses TLR2-induced chondrocyte dysfunction and attenuates age-related osteoarthritis. *Proc. Natl. Acad. Sci. USA* **120**, e2207993120 (2023).
70. Zhang, Y. et al. CC chemokines and receptors in osteoarthritis: new insights and potential targets. *Arthritis Res. Ther.* **25**, 113 (2023).
71. Dunn, S. L. et al. Gene expression changes in damaged osteoarthritic cartilage identify a signature of non-chondrogenic and mechanical responses. *Osteoarthr. Cartil.* **24**, 1431–1440 (2016).
72. James, A. W. et al. NELL-1 in the treatment of osteoporotic bone loss. *Nat. Commun.* **6**, 7362 (2015).
73. Li, C. et al. Nell-1 Is a key functional modulator in osteochondrogenesis and beyond. *J. Dent. Res.* **98**, 1458–1468 (2019).
74. Hamdan, Y. et al. LRRC15, a potential key player in cartilage ossification in osteoarthritis disease. *Osteoarthr. Imaging* **4**, 100215 (2024).
75. Wang, C. et al. Type III collagen is a key regulator of the collagen fibrillar structure and biomechanics of articular cartilage and meniscus. *Matrix Biol.* **85–86**, 47–67 (2020).
76. Behrendt, P. et al. IL-10 reduces apoptosis and extracellular matrix degradation after injurious compression of mature articular cartilage. *Osteoarthr. Cartil.* **24**, 1981–1988 (2016).
77. Attur, M. et al. Periostin loss-of-function protects mice from post-traumatic and age-related osteoarthritis. *Arthritis Res Ther.* **23**, 104 (2021).
78. Tillgren, V., Ho, J. C. S., Önnerfjord, P. & Kalamajski, S. The novel small leucine-rich protein chondroadherin-like (CHADL) is expressed in cartilage and modulates chondrocyte differentiation. *J. Biol. Chem.* **290**, 918–925 (2015).
79. Tscheudschilsuren, G. et al. Regulation of mesenchymal stem cell and chondrocyte differentiation by MIA. *Exp. Cell Res* **312**, 63–72 (2006).
80. Li, Z. et al. Single-cell RNA sequencing reveals the difference in human normal and degenerative nucleus pulposus tissue profiles and cellular interactions. *Front. Cell Dev. Biol.* **10**, 910626 (2022).
81. Nanus, D. E. et al. Synovial tissue from sites of joint pain in knee osteoarthritis patients exhibits a differential phenotype with distinct fibroblast subsets. *EBioMedicine* **72**, 103618 (2021).
82. Wangler, S. et al. CD146/MCAM distinguishes stem cell subpopulations with distinct migration and regenerative potential in degenerative intervertebral discs. *Osteoarthr. Cartil.* **27**, 1094–1105 (2019).
83. Fan, W. et al. CD105 promotes chondrogenesis of synovium-derived mesenchymal stem cells through Smad2 signaling. *Biochem. Biophys. Res. Commun.* **474**, 338–344 (2016).
84. Matta, C. et al. Molecular phenotyping of the surfaceome of migratory chondroprogenitors and mesenchymal stem cells using biotinylation, glycocapture and quantitative LC-MS/MS proteomic analysis. *Sci. Rep.* **9**, 9018 (2019).
85. Cleary, M. A. et al. Expression of CD105 on expanded mesenchymal stem cells does not predict their chondrogenic potential. *Osteoarthr. Cartil.* **24**, 868–872 (2016).
86. Guo, H. et al. CD73 alleviates osteoarthritis by maintaining anabolism and suppressing catabolism of chondrocytes extracellular matrix. *J. Orthop. Transl.* **49**, 96–106 (2024).

87. Newton, P. T. et al. A radical switch in clonality reveals a stem cell niche in the epiphyseal growth plate. *Nature* **567**, 234–238 (2019).
88. Oichi, T. et al. Nutrient-regulated dynamics of chondroprogenitors in the postnatal murine growth plate. *Bone Res* **11**, 20 (2023).
89. Kong, Y. et al. Role of complement factor D in cardiovascular and metabolic diseases. *Front. Immunol.* **15**, 1453030 (2024).
90. Banda, N. K. et al. Role of C3a receptors, C5a receptors, and complement protein C6 deficiency in collagen antibody-induced arthritis in mice. *J. Immunol.* **188**, 1469–1478 (2012).
91. Collins, K. H. et al. Adipose-derived leptin and complement factor D mediate osteoarthritis severity and pain. *Sci. Adv.* **11**, eadt5915 (2025).
92. Chou, W.-C. et al. Galectin-3 facilitates inflammation and apoptosis in chondrocytes through upregulation of the TLR-4-mediated oxidative stress pathway in TC28a2 human chondrocyte cells. *Environ. Toxicol.* **37**, 478–488 (2022).
93. Weinmann, D. et al. Galectin-3 induces a pro-degradative/ inflammatory gene signature in human chondrocytes, teaming up with galectin-1 in osteoarthritis pathogenesis. *Sci. Rep.* **6**, 39112 (2016).
94. Justo, B. L. & Jasiulionis, M. G. Characteristics of TIMP1, CD63, and β1-Integrin and the functional impact of their interaction in cancer. *Int J. Mol. Sci.* **22**, 9319 (2021).
95. Noble, M. & Pröschel, C. The many roles of C1q. *eLife* **9**, e61599 (2020).
96. Scott-Hewitt, N. et al. Microglial-derived C1q integrates into neuronal ribonucleoprotein complexes and impacts protein homeostasis in the aging brain. *Cell* **187**, 4193–4212.e24 (2024).
97. Zhen, G. et al. Inhibition of TGF-β signaling in mesenchymal stem cells of subchondral bone attenuates osteoarthritis. *Nat. Med* **19**, 704–712 (2013).
98. Muratovic, D. et al. Elevated levels of active transforming growth factor β1 in the subchondral bone relate spatially to cartilage loss and impaired bone quality in human knee osteoarthritis. *Osteoarthr. Cartil.* **30**, 896–907 (2022).
99. Arai, F., Ohneda, O., Miyamoto, T., Zhang, X. Q. & Suda, T. Mesenchymal stem cells in perichondrium express activated leukocyte cell adhesion molecule and participate in bone marrow formation. *J. Exp. Med* **195**, 1549–1563 (2002).
100. Wu, C.-L., Harasymowicz, N. S., Klimak, M. A., Collins, K. H. & Guilak, F. The role of macrophages in osteoarthritis and cartilage repair. *Osteoarthr. Cartil.* **28**, 544–554 (2020).
101. Maldonado, M. & Nam, J. The role of changes in extracellular matrix of cartilage in the presence of inflammation on the pathology of osteoarthritis. *Biomed. Res. Int.* **2013**, 284873 (2013).
102. Hiruthyaswamy, S. P. et al. Molecular signaling pathways in osteoarthritis and biomaterials for cartilage regeneration: a review. *Bioengineered* **16**, 2501880 (2025).
103. Kular, J. K., Basu, S. & Sharma, R. I. The extracellular matrix: Structure, composition, age-related differences, tools for analysis and applications for tissue engineering. *J. Tissue Eng.* **5**, 2041731414557112 (2014).
104. Li, H. et al. TSP-1 increases autophagy level in cartilage by upregulating HSP27 which delays progression of osteoarthritis. *Int. Immunopharmacol.* **128**, 111475 (2024).
105. Mitchell, R. A. et al. Macrophage migration inhibitory factor (MIF) sustains macrophage proinflammatory function by inhibiting p53: regulatory role in the innate immune response. *Proc. Natl. Acad. Sci. USA* **99**, 345–350 (2002).
106. Hou, S.-M. et al. CXCL1 contributes to IL-6 expression in osteoarthritis and rheumatoid arthritis synovial fibroblasts by CXCR2, c-Raf, MAPK, and AP-1 pathway. *Arthritis Res. Ther.* **22**, 251 (2020).
107. Chwastek, J., Kędziora, M., Borczyk, M., Korostyński, M. & Starowicz, K. Inflammation-driven secretion potential is upregulated in osteoarthritic fibroblast-like synoviocytes. *Int J. Mol. Sci.* **23**, 11817 (2022).
108. Luo, H., Li, L., Han, S. & Liu, T. The role of monocyte/macrophage chemokines in pathogenesis of osteoarthritis: a review. *Int J. Immunogenet.* **51**, 130–142 (2024).
109. Hu, T. et al. CD99 mediates neutrophil transmigration through the bEnd.3 monolayer via the induction of oxygen-glucose deprivation. *Biochem. Biophys. Res. Commun.* **526**, 799–804 (2020).
110. Nigro, P., Pompilio, G. & Capogrossi, M. C. Cyclophilin a: a key player for human disease. *Cell Death Dis.* **4**, e888 (2013).
111. Ansari, M. Y., Ahmad, N. & Haqqi, T. M. Oxidative stress and inflammation in osteoarthritis pathogenesis: role of polyphenols. *Biomed. Pharmacother.* **129**, 110452 (2020).
112. Guo, L. et al. Role of Angptl4 in vascular permeability and inflammation. *Inflamm. Res.* **63**, 13–22 (2014).
113. Neumaier, E. E., Rothhammer, V. & Linnerbauer, M. The role of midkine in health and disease. *Front. Immunol.* **14**, 1310094 (2023).
114. Dudley, A. C. & Griffioen, A. W. Pathological angiogenesis: mechanisms and therapeutic strategies. *Angiogenesis* **26**, 313–347 (2023).
115. Hermann, L. M. et al. Angiopoietin-like-4 is a potential angiogenic mediator in arthritis. *Clin. Immunol.* **115**, 93–101 (2005).
116. Allen, K. D. et al. Racial differences in self-reported pain and function among individuals with radiographic hip and knee osteoarthritis: the Johnston County Osteoarthritis Project. *Osteoarthr. Cartil.* **17**, 1132–1136 (2009).
117. Vaughn, I. A., Terry, E. L., Bartley, E. J., Schaefer, N. & Fillingim, R. B. Racial-ethnic differences in osteoarthritis pain and disability: a meta-analysis. *J. Pain.* **20**, 629–644 (2019).
118. Bolander, J. et al. The synovial environment steers cartilage deterioration and regeneration. *Sci. Adv.* **9**, eade4645 (2023).

Acknowledgements

This study was supported by NIH grants R01 DE031413 (MB), and P30 AR072571 (TN). Funding: The authors declare that they have no financial interests regarding the content of this manuscript.

Author contributions

R.D.R. performed the experiments and analyzed the data with the help of A.K.C. and M.V.B. T.N., B.S., T.P.S., M.A., M.W.G., C.Z., and M.V.B. helped with conception, interpretation, and manuscript editing. M.V.B. conceived and designed the study. R.D.R., M.V.B., B.S., and M.W.G. interpreted the data and wrote the manuscript.

Competing interests

The authors declare no competing interests.

Additional information

Supplementary information The online version contains supplementary material available at https://doi.org/10.1038/s42003-025-08586-8.

Correspondence and requests for materials should be addressed to Manish V. Bais.

Peer review information *Communications Biology* thanks the anonymous reviewers for their contribution to the peer review of this work. Primary Handling Editors: Eirini Trompouki and Joao Valente. A peer review file is available.